A role for the peroxisomal 3-ketoacyl-CoA thiolase B enzyme in the control of PPARα-mediated upregulation of SREBP-2 target genes in the liver.

Marco Fidaleo, Ségolène Arnauld, Marie-Claude Clémencet, Grégory Chevillard, Marie-Charlotte Royer, Melina de Bruycker, Ronald J. A. Wanders, Anne Athias, Joseph Gresti, Pierre Clouet, et al.

▶ **To cite this version:**

Marco Fidaleo, Ségolène Arnauld, Marie-Claude Clémencet, Grégory Chevillard, Marie-Charlotte Royer, et al.. A role for the peroxisomal 3-ketoacyl-CoA thiolase B enzyme in the control of PPARα-mediated upregulation of SREBP-2 target genes in the liver.: ThB and cholesterol biosynthesis in the liver. Biochimie, 2011, 93 (5), pp.876-91. 10.1016/j.biochi.2011.02.001 . inserm-00573373

HAL Id: inserm-00573373

https://inserm.hal.science/inserm-00573373

Submitted on 3 Mar 2011

HAL is a multi-disciplinary open access archive for the deposit and dissemination of scientific research documents, whether they are published or not. The documents may come from teaching and research institutions in France or abroad, or from public or private research centers.

L'archive ouverte pluridisciplinaire **HAL**, est destinée au dépôt et à la diffusion de documents scientifiques de niveau recherche, publiés ou non, émanant des établissements d'enseignement et de recherche français ou étrangers, des laboratoires publics ou privés.

A role for the peroxisomal *3-ketoacyl-CoA thiolase B* enzyme in the control of PPARα-mediated upregulation of SREBP-2 target genes in the liver

Marco Fidaleo[1,2,8#], Ségolène Arnauld[1,2#], Marie-Claude Clémencet[1,2], Grégory Chevillard[1,2,9], Marie-Charlotte Royer[1,2], Melina De Bruycker[3], Ronald J.A. Wanders[4], Anne Athias[5], Joseph Gresti[1,6], Pierre Clouet[1,6], Pascal Degrace[1,6], Sander Kersten[7], Marc Espeel[3], Norbert Latruffe[1,2], Valérie Nicolas-Francès[1,2] and Stéphane Mandard[1,2,*]

[1]Centre de recherche INSERM U866, Dijon, F-21000, France; [2]Université de Bourgogne, Faculté des Sciences Gabriel, Equipe Biochimie Métabolique et Nutritionnelle, Dijon, F-21000, France; [3]Department of Human Anatomy, Embryology, Histology and Medical Physics, Ghent University, Ghent, Belgium; [4]Laboratory Genetic Metabolic Diseases, Academic Medical Center at the University of Amsterdam, Meibergdreef 9, 1105 AZ Amsterdam, the Netherlands. [5]Université de Bourgogne, IFR100, Plateau Technique de Lipidomique - Dijon, France. [6]INSERM U866, Equipe Physiopathologie des dyslipidémies, Faculté des Sciences Gabriel, 21000 Dijon, France; [7]Nutrition, Metabolism and Genomics group, Division of Human Nutrition, Wageningen University, Wageningen, The Netherlands. [8]Present address: Department of Cellular and Developmental Biology, University of Rome “La Sapienza”, P.le Aldo Moro 5, 00185 Rome, Italy. [9]Present address: Lady Davis Institute for Medical Research, McGill University, 3755 Côte Ste. Catherine Road, Montreal, QC H3T 1E2, Canada;

*corresponding author : Stéphane MANDARD (PhD), LBMN, centre de recherche INSERM U866, 6, Boulevard Gabriel, 21000 Dijon, France. Phone: (+33) 3 80 39 62 02, Fax: (+33) 3 80 39 62 50, E-mail: stephane.mandard@u-bourgogne.fr

[#] these authors contributed equally to this work.

Short title: ThB and cholesterol biosynthesis in the liver

Keywords: peroxisomal 3-ketoacyl-CoA thiolase B, PPARα, cholesterol, Wy14,643, Fatty Acid Oxidation.

Abstract

Peroxisomal *3-ketoacyl-CoA thiolase B* (*Thb*) catalyzes the final step in the peroxisomal β-oxidation of straight-chain acyl-CoAs and is under the transcription control of the nuclear hormone receptor PPARα. PPARα binds to and is activated by the synthetic compound Wy14,643 (Wy). Here, we show that the magnitude of Wy-mediated induction of peroxisomal β-oxidation of radiolabeled (1-^{14}C) palmitate was significantly reduced in mice deficient for *Thb*. In contrast, mitochondrial β-oxidation was unaltered in *Thb*$^{-/-}$ mice. Given that Wy-treatment induced Acox1 and MFP1/2 activity at a similar level in both genotypes, we concluded that the thiolase step alone was responsible for the reduced peroxisomal β-oxidation of fatty acids. Electron microscopic analysis and cytochemical localization of catalase indicated that peroxisome proliferation in the liver after Wy-treatment was normal in *Thb*$^{-/-}$ mice. Intriguingly, microarray analysis revealed that mRNA levels of genes encoding for cholesterol biosynthesis enzymes were upregulated by Wy in Wild-Type (WT) mice but not in *Thb*$^{-/-}$ mice, which was confirmed at the protein level for the selected genes. The non-induction of genes encoding for cholesterol biosynthesis enzymes by Wy in *Thb*$^{-/-}$ mice appeared to be unrelated to defective SREBP-2 or PPARα signalling. No difference was observed in the plasma lathosterol/cholesterol ratio (a marker for *de novo* cholesterol biosynthesis) between Wy-treated WT and *Thb*$^{-/-}$ mice, suggesting functional compensation. Overall, we conclude that ThA and SCPx/SCP2 thiolases cannot fully compensate for the absence of ThB. In addition, our data indicate that ThB is involved in the regulation of genes encoding for cholesterol biosynthesis enzymes in the liver, suggesting that the peroxisome could be a promising candidate for the correction of cholesterol imbalance in dyslipidemia.

Introduction

Over the last decade, considerable effort has been made to disentangle the various pathways in which peroxisomes are involved. Evidence abounds that defects in peroxisome biogenesis and β-oxidation of fatty acids cause several inherited diseases, which - in most cases - are lethal [1]. Peroxisomes are known to be involved in many aspects of lipid metabolism, including synthesis of bile acids and plasmalogens, synthesis of cholesterol and isoprenoids, α-oxidation and β-oxidation of very-long-straight- or -branched-chain acyl-CoAs. The peroxisomal degradation of straight-chain acyl-CoAs by a discrete set of enzymes has been well documented. The β-oxidation of straight-chain acyl-CoAs starts with a reaction catalyzed by acyl-CoA oxidase 1 (Acox1), the rate-limiting enzyme of the β-oxidation pathway. This step is followed by two enzymatic reactions carried out by the MFP1/L-bifunctional protein and the MFP2/D-bifunctional protein. The fourth and last step is catalyzed by the peroxisomal 3-ketoacyl-CoA thiolases.

Intriguingly, two different peroxisomal 3-ketoacyl-CoA thiolases for very-long-straight-chain fatty acids (thiolase A, ThA, Acaa1a and thiolase B, ThB, Acaa1b, EC:2.3.1.16) have been cloned in rodents, while only one corresponding gene (peroxisomal 3-acetyl-CoA acetyltransferase-1, ACAA1) has been identified in humans [2-4]. The third peroxisomal thiolase, SCP-2/3-ketoacyl-CoA thiolase (SCPx), displays a very broad substrate specificity, including cleavage of 2-methyl branched as well as straight-chain 3-ketoacyl-CoA esters [1, 5, 6].

Targeted disruption of the mouse *Acox1* gene has revealed the critical role of this enzyme in hepatocellular proliferation and peroxisome proliferation as well as in the catabolism of very-long-chain fatty acids [7, 8]. Peroxisomal acyl-CoA oxidase deficiency and its consequences are also well documented in humans [9]. Two isoforms of ACOX1 (a and b) have been characterized in mouse and man [10]. Vluggens *et al.* recently studied the respective roles of these isoforms by using adenovirally driven hACOX-1a and hACOX-1b in *Acox1* null mice [10, 11]. The hACOX-1b isoform was more effective in reversing the *Acox1* null phenotype than the hACOX-1a isoform, illustrating functional differences between these two closely related proteins. Other reports aimed

at characterizing the consequences of *Mfp-1* (L-PBE) and/or *Mfp-2* (D-PBE) deficiencies in mice are also available [12]. While most biochemical parameters remained unaffected by the single deletion of *Mfp*-1, *Mfp-1* deficient mice displayed marked reduction in peroxisome proliferation when challenged with a peroxisome proliferator [13]. The *Mfp-2* deficient mice displayed disturbances in bile acid metabolism and in the breakdown of very-long-chain fatty acids. Recently, it was also reported that deletion of *Mfp-2* in mice resulted in the combined upregulation of PPARalpha and SREBP-2 target genes in the liver, suggesting a potential cross-talk between the two signalling cascades, orchestrated by MFP-2 [14].

Information about ACAA1 remains fragmentary and only a limited number of studies has been reported so far [4, 15]. The discovery of a young girl with a specific mutation within the *ACAA1* gene was initially believed to shed some light on the role of ACAA1 in very-long-chain fatty acid catabolism [16]. However, follow-up investigations demonstrated that the true defect was rather at the level of D-bifunctional protein, rendering the impact of ACAA1 in humans uncertain [15]. To date, it is not clear if ACAA1 plays a similar role in humans and rodents, nor whether ACAA1 can be considered as the ortholog of ThA and/or ThB [2]. Hence, in an effort to improve our understanding of the functions of peroxisomal 3-ketoacyl-CoA thiolases, we began by studying the deletion of *Thb* in mice [17].

As a hypolipidemic fibrate drug, the synthetic peroxisome proliferator Wy14,643 (Wy) causes proliferation of peroxisomes in liver parenchymal cells [18]. In WT mice, Wy administration gives rise to a robust elevation of mitochondrial and peroxisomal fatty acid β-oxidation, hepatocyte hyperplasia and then hepatomegaly, but these effects are not found in PPARα deficient mice [19]. At the molecular level, Wy has been characterized as a potent and selective activator of the nuclear hormone receptor PPARα in humans and rodents [20, 21]. PPARα is well expressed in metabolically active tissues such as hepatic, renal and brown adipose tissue [22]. After binding of Wy, PPARα becomes activated and regulates the expression of a subset of genes commonly referred to as PPARα target genes [23]. Previously, *Thb* was identified as a gene highly responsive

to PPARα agonists [24, 25]. Therefore *Thb* mRNA levels can be modulated by treatment with peroxisome proliferators (PP). In addition to being crucial for lipid handling, PPARα has been linked to the regulation of genes involved in cell growth, differentiation and inflammation control [26-29]. Using gene expression profiling combined with northern-blotting or RT-qPCR experiments, it has also been established that the effects of Wy on hepatic gene expression are robust and almost exclusively mediated by PPARα [30, 31].

Since *Thb* expression is highly activated by PPARα, it can be hypothesized that the effect of *Thb* deletion would be more pronounced under conditions of PPARα activation. Accordingly, the effect of *Thb* deletion was studied in WT mice and *Thb*$^{-/-}$ mice, both treated with Wy for 8 days, and fasted for 6h before sacrifice. The results indicate that *ThB* inactivation is associated with a modest but statistically significant decrease in peroxisomal palmitate β-oxidation. It is also worth noting that ThB is dispensable for Wy-mediated cell and peroxisome proliferation in the liver. Intriguingly, the Wy-induction of some genes encoding for cholesterol biosynthesis enzymes was altered in *Thb*$^{-/-}$ mice, suggesting that ThB has a unique and unexpected role in cholesterol metabolism.

2. Materials and methods

2.1. Animals

Male, pure-bred Sv129 (WT) and *Thb*$^{-/-}$ mice have been previously described [17]. Mice were kept in normal cages with food and water *ad libitum*, unless indicated. Mice were routinely fed a standard commercial pellet diet (UAR A03-10 pellets from Usine d'Alimentation Rationnelle, Epinay sur Orge, France, 3.2 kcal/g) consisting (by mass) about 5.1% fat (C16:0 0.89% ; C16:1n-7 ±0.09% ; C18:0 ±0.45% ; C18:1n-9 ±1.06%, C18:2n-9 ±1.53% and traces of C18:3n-9). At the time of sacrifice, animals were around 4–5 months old. Unless indicated, male mice in the fasted state were deprived of food for 6h starting at 4:0 pm. Blood was collected *via* orbital puncture into EDTA tubes. The animal experiments were approved by the animal experimentation committee of

the University of Burgundy (protocol number n°1904) and were performed according to European Union guidelines for animal care.

2.2. Chemicals

For the purposes of the present work, Wy was obtained from ChemSyn Laboratories (Lenexa, Kansas), Fenofibrate from Sigma, Arabic gum from Merck, qPCR MasterMix Plus for SYBR Green I with fluorescein from Eurogentec, and (1-^{14}C) palmitate from Amersham Biosciences.

2.3. Pharmacological protocol

Male mice were treated by intragastric gavage with two kinds of peroxisome proliferators: (1) Wy (30 mg/kg/day, approximately 200 µl/dose) for 8 days, and (2) fenofibrate (100 mg/kg/day, 200 µl/day) for 14 days. In both cases, these molecules were dispersed into water containing 3% Arabic gum. This protocol was performed daily between 8.00 a.m. and 10.00 a.m. Livers were excised, weighed, snap-frozen in liquid nitrogen, and stored at -80 °C. For the RNA analyses, tissue samples were taken from the same liver lobe in each mouse to avoid variability.

2.4. Peroxisomal and mitochondrial oxidation of (1-^{14}C) palmitate

Peroxisomal and mitochondrial oxidation of (1-^{14}C) palmitate were measured as described elsewhere [32]. However, instead of quantifying the $^{14}CO_2$ radioactivity level, the release of (1-^{14}C) acetyl-CoA and (1-^{14}C) acetyl-carnitine in perchloric acid was quantified after one cycle of β-oxidation.

2.5. Mitochondrial and peroxisomal enzyme assays.

Liver homogenates and mitochondrial fractions were prepared as usually described [33]. Livers were homogenized with a Teflon pestle rotating at 300 rpm in a cooled Potter-Elvehjem homogenizer, in 20 volumes of chilled solution of 0.25 M sucrose, 2 mM EGTA, and 10 mM Tris-HCl (pH 7.4). Palmitate oxidation rates were measured in two separate media: the first allowed

both mitochondrial and peroxisomal activities to occur, and the second allowed only peroxisomal activity. The functional state of mitochondria was estimated by the differential activities of monoamine oxidase (EC 1.4.3.4) and of citrate synthase (EC 4.1.3.7), whereas that of peroxisomes were determined by CN-insensitive palmitoyl-CoA-dependent NAD+ reduction, which has been defined as the "peroxisomal fatty acid oxidizing system" (PFAOS) [34-36]. Carnitine palmitoyltransferase I alpha (CPT-Iα) activity was measured using L-(^{3}H)carnitine (92.5 GBq/mol; Amersham Biosciences TRK762) with palmitoyl-CoA, as described elsewhere [32].

2.6. Cytochemical localization of catalase and peroxisome electron microscopy

Peroxisomes were identified in liver sections at light and electron microscopy levels, thereby revealing the enzymatic activity of catalase, the main peroxisomal marker enzyme, according to established procedures [37, 38]. Liver samples were fixed in a 4% formaldehyde, 0.1M sodiumcacocylate buffer (pH 7.3) containing 1% (w/v) calcium chloride for 24 h at room temperature, after which sections (60 μm) were cut with a cryostat. The cryostat sections were then incubated in a diaminobenzidine (DAB)-hydrogenperoxide medium at pH 10.5 (Theorell-Stenhagen buffer) for 3 hours at 25°C. After DAB-incubation, the sections were rinsed, post-osmicated and embedded in epoxy resin (LX-112) following standard protocols. Semi-thin (2 μm) sections were cut for light microscopy, and ultra-thin (750 nm) sections for electron microscopy.

2.7. Histochemistry/Histology.

We kindly acknowledge the expertise of Amandine Bataille (Plateau technique d'imagerie cellulaire CellImaP, IFR 100 Santé-STIC, Dijon, France) for liver sections and staining with hematoxylin and eosin.

2.8. In vivo proliferation assay of liver cells

After sacrifice of the animals, liver samples were taken from each treatment group. The samples were placed in 4 % formalin overnight, incubated in 70 % ethanol and dehydrated through a graded

series of alcohol (80%-100%). Finally, liver samples were placed in xylene before being embedded in paraffin. Paraffin sections (4 μm thick) were cut and fixed to polylysine-coated slides. Proliferative activity was then measured by labeling of the Ki-67 antigen, which is expressed in the nuclei of all cells in G1, S, G2, and M phases. After removing paraffin with xylene, sections were re-hydrated in a graded series of ethanol from 100% to 95%. Endogenous peroxidase was blocked with 3°/°° H_2O_2 in methanol for 10 min. All sections were pre-treated in a microwave oven in a 10 mM citrate buffer at pH = 6 for 10 minutes at 100°C. Non-specific binding sites were blocked using 10% goat serum (diluted in PBS 0.1% and triton X-100) before an incubation of 2 h at room temperature. Incubation with anti-Ki-67 (AB9260, Millipore), the primary polyclonal antibody, was then performed, followed by incubation with a goat anti-rabbit IgG secondary antibody (Santa Cruz Biotechnology, sc-2004). Ki-67 positive cells were visualized by exposing the peroxidase to 3,3'-diaminobenzidine hydrochloride chromogen substrate (DAKO, K3467, France) following by counterstaining with hematoxylin. Slides were then washed with deionized water and mounted with a permanent medium (Clearmount mounting solution, Invitrogen Ltd., cat. no. 00-8010). It is also worth noting that all cells in the active phases of the cell cycle stained brown except G0-phase cells, which remained blue. To determine mitotic activity, an average of 4 fields on each slide was analysed per animal (n=3). The Ki-67 labelling index was defined as Ki-67 positive cells/total cells present in the field.

2.9. Plasma metabolites

Plasma was initially collected into EDTA tubes *via* retro-orbital punctures and then centrifuged at 4°C (10 min, 6000 rpm). Plasma β-hydroxybutyrate levels were determined using a β-hydroxybutyrate-FS kit (Diasys Diagnostic Systems International, France). Plasma free fatty acid levels were evaluated with the NEFA-C kit from WAKO.

For lathosterol measurements, plasma was mixed with epicoprostanol, which was used as a control standard. Potassium hydroxide saponification was followed by lipid extraction with hexane. Cholesterol and lathosterol were analyzed in the trimethylsilyl ether state by GC-MS using a

Hewlett Packard HP6890 Gas Chromatograph equipped with an HP7683 Injector and an HP5973 Mass Selective Detector.

3.0. RNA isolation and reverse transcription step

Liver RNA was extracted with a TRIzol reagent (Invitrogen) using the supplier's instructions. RNA was then further purified (from free nucleotides and contaminating genomic DNA) using RNeasy columns (Qiagen) and DNAse treatment. 1 μg of RNA was used for reverse transcription with iScript Reverse Transcriptase (Bio-rad).

3.1. Oligonucleotide microarray

Liver RNA samples, prepared using a TRIzol reagent, were collected from four groups of five mice. One group of 5 WT mice and one group of 5 *Thb*$^{-/-}$ mice had been treated with Wy, the other two groups (5 WT mice and 5 *Thb*$^{-/-}$ mice) had not been treated with Wy. An equivalent amount of RNA from each animal (from all four groups) was subsequently pooled. Pooled RNA was further purified using Qiagen RNeasy columns and the quality was verified using an Agilent bioanalyzer 2100 (Agilent technologies, Amsterdam, the Netherlands). RNA was judged suitable for array hybridization if the sample showed intact bands corresponding to the 18S and 28S rRNA subunits and no chromosomal peaks. As in a previous study, 10 μg of RNA was used for one cycle of cRNA synthesis (Affymetrix, Santa Clara, USA) [39]. Hybridization, washing and scanning of Affymetrix GeneChip mouse genome 430 2.0 arrays were performed following standard Affymetrix protocols. Fluorimetric data were processed by Affymetrix GeneChip Operating software, and the gene chips were globally scaled to all probe sets with an identical target intensity value. Further analysis was performed using Data Mining Tools (Affymetrix).

3.2. Real-Time Quantitative PCR

PCR reactions were performed using the qPCR MasterMix Plus for SYBR Green I with fluorescein (Eurogentec). All PCR reactions were performed with MultiGuard Barrier Tips (Sorenson

BioScience, Inc.) and an iCycler PCR machine (Bio-Rad Laboratories). Primers were designed to generate a PCR amplification product of 50-120 bp and were selected following the recommendations provided with the Primer 3 software (http://frodo.wi.mit.edu/cgi-bin/primer3/primer3_www.cgi). The specificity of the amplification was verified *via* melt curve analysis, and the efficiency of PCR amplification was evaluated by a standard curve procedure. The expression of each gene was determined relative to 36B4 as a control gene and the relative gene expression was calculated by using the "delta-delta Ct" quantification method.

3.3. Preparation of liver nuclear extracts

Nuclear extracts of liver were prepared following established protocols [40].

3.4. Immunoblot analysis

10 μg of nuclear protein was separated on a 10% (w/v) polyacrylamide gel in the presence of 0.1% (w/v) SDS and transferred on to PVDF membranes. A broad range pre-stained SDS-PAGE standard (Bio-Rad, 161-0318) was used as a protein ladder in this study. After membrane saturation at room temperature for 90 minutes with TBS (0.1 M Tris-HCl , pH 8.0, 0.15 M NaCl) containing 0.1% (v/v) Tween 20 and 5% (w/v) fat-free milk, blots were then incubated overnight at 4°C with a polyclonal rabbit antibody against HMG-CoA reductase (sc-33827, 1:200, Santa Cruz Biotechnology); a polyclonal anti-actin rabbit antibody (A2066, 1:5000, Sigma); a polyclonal anti-SREBP-2 rabbit antibody (Ab28482, 1:200, Abcam); a polyclonal anti-PPARα rabbit antibody (sc-9000, Santa Cruz Biotechnology); a monoclonal mouse antibody against the TATA-binding protein (Ab818,1:2000, Abcam); and a polyclonal sheep antibody to histone H1 (Ab1938, Abcam), respectively. High affinity purified antibodies reacting against phosphomevalonate kinase (Pmvk, 1:500) and mevalonate kinase (Mvk, 1:1000) have been characterized elsewhere [41]. Similarly, the polyclonal rabbit antibody reacting against both thiolase A and B proteins (PTL, 1:15000) and the mouse antibody reacting against Acox1 (1:200) have also been previously characterized [41-43]. After three washes in TBS containing 0.1% (v/v) Tween 20, primary antibodies were detected

using a peroxidase-conjugated IgG antibody, the choice of which depends on the primary antibody of interest: a goat anti-rabbit IgG Antibody, (1:30000, sc-2004, Santa Cruz Biotechnology), a goat anti-mouse IgG antibody, (1:30000, Sc-2005, Santa Cruz Biotechnology) or a rabbit anti-sheepIgG antibody (Ab6747, Abcam). The protein bands labelled with the antibodies were visualized using a Western-blotting chemiluminescence luminol reagent (Santa Cruz Biotechnology) by exposure to X-ray films (Amersham). Densitometry of proteins on Western blots was performed using the Scion Image software.

3.5. Liver cholesterol

About 100 mg of each liver sample was saponified by heating in ethanol-KOH, and then cholesterol was extracted from the saponified solution with hexane. Epicoprostanol (5β-cholestan-3α-ol) was used as a standard. After evaporation of hexane, cholesterol was converted to trimethylesters using bis-silyl-trifluoracetamide. Hepatic total cholesterol was subsequently quantified by gas chromatography. To measure cholesterol ester levels, Folch extraction was followed by a silylation step using bis (trimethyl-silyl) trifluoro-acetamide. Free cholesterol concentration was taken to be the difference between total and esterified cholesterol.

3.6. Statistical analyses

Data are presented as means with their standard errors. The effects of genotype (KO vs WT), of treatment (with or without Wy), and of genotype-treatment interaction were evaluated using a two-way ANOVA test. The cut-off for statistical significance was set at a p-value of 0.05.

4. Results

4.1. Peroxisomal palmitate oxidation is reduced in Wy-treated Thb$^{-/-}$ mice

As previously shown, we found that *Thb* expression was strongly induced by Wy (Fig. 1a). Interestingly, *Tha* expression was higher in *Thb*$^{-/-}$ mice treated with Wy (Wy-genotype interaction,

p=0.046), indicating a possible compensation of the non-expression of the *thb* gene (Fig. 1a). A Western-blotting experiment performed with an antibody unable to distinguish between ThA and ThB isotypes confirmed the hepatic enrichment of ThA in *Thb*$^{-/-}$ mice treated with Wy (Fig. 1b). When compared to WT mice, the *Acox1*, *Mfp-1* and *Scpx/Scp2* thiolase mRNA levels were clearly higher in *Thb*$^{-/-}$ mice, and statistically significant at face value (p=0.0506; p=0.017; p=0.0506 for *Acox1*, *Mfp-1* and *Scpx/Scp2*, respectively). After treatment with Wy, the *Mfp-1 mRNA* level was significantly higher in *Thb*$^{-/-}$ mice (Wy-genotype interaction, p=0.004), while the *Scpx/Scp2* thiolase and *Acox1* mRNA levels increased in a similar way (which was further confirmed at the protein level for Acox1, Fig. 1d) (Fig. 1c, p=0.252). To determine whether lack of *Thb* in mice translates into functional alteration of fatty acid β-oxidation, we measured the rate of peroxisomal β-oxidation of (1-^{14}C) palmitate, using a liver homogenate from each mouse, both WT and *Thb*$^{-/-}$, with and without Wy-treatment (Fig. 1f). The effect of *Thb* deletion on the peroxisomal β-oxidation of (1-^{14}C) palmitate was Wy-sensitive (Wy-genotype interaction, p=0.0035), indicating that the deletion of *Thb* leads to a significant decrease (-31%) in the induction of β-oxidation. *Thb* inactivation did not affect the production of NADH (which shows the enzymatic activity of Acox1 and MFP-1/MFP-2) regardless of the treatment conditions (Fig. 1g). It is therefore clear that ThA and SCPx thiolases cannot fully compensate for ThB when *Thb*$^{-/-}$ mice are metabolically challenged by the increase in fatty acid oxidation that Wy induces.

4.2. Lack of ThB does not affect mitochondrial palmitate oxidation

Although *Thb* deletion caused a reduced rate of peroxisomal palmitate β-oxidation, it had no effect on mitochondrial palmitate oxidation in Wy-treated *Thb*$^{-/-}$ mice, as shown by the results for the liver homogenate (Fig. 2a), and for the liver mitochondrial fraction (Fig. 2b). Consistent with these data, mRNA levels, the activities of Carnitine Palmitoyl Transferase-Iα (CPT-Iα) and of the two mitochondrial markers, MonoAmine Oxidase (MAO) and Citrate Synthase (CS) were similar for

WT mice and *Thb*$^{-/-}$ mice (Table 1 and supplemental Table 1). Additionally, circulating free fatty acids (FFA) and β-hydroxybutyrate levels were not significantly altered in *Thb*$^{-/-}$ mice, both with and without Wy-treatment, or after 24 h-fasting (Table 1). Taken together, the data show that *Thb* deletion has very little impact on mitochondrial fatty acid β-oxidation, but that it has a negative effect on peroxisomal fatty acid β-oxidation when mice are metabolically challenged.

4.3. Wy-treated *Thb*$^{-/-}$ mice display hepatomegaly similar to WT mice

Besides alteration of lipid metabolism, the knockout of the *Acox1* gene in mice is widely acknowledged to be associated with major hepatomegaly combined with the absence of peroxisomes [7]. In order to check for the possible impact of *Thb* deletion on hepatomegaly, the relative liver mass was evaluated for both genotypes. The hepatosomatic index was significantly lower in *Thb*$^{-/-}$ mice than in WT mice (p=0.0136) (Fig. 3a). After Wy-treatment, the hepatosomatic index increased in mice of both genotypes, although less in *Thb*$^{-/-}$ mice, suggesting the possible involvement of ThB in Wy-induced hepatomegaly (Wy-genotype interaction, p=0.004). To further investigate the putative role of ThB in hepatocyte proliferation, the size and number of liver cells were quantified by histological staining using hematoxylin and eosin. Both parameters were affected by Wy: cell numbers decreased and cell surface increased. No genotype effect *per se* was observed either for cell number (p=0.105) or cell surface (p=0.250) (Fig.3b), suggesting that *Thb* deletion has no marked effect on liver cell morphology (Fig. 3c). To assess the possible implication of ThB in liver cell proliferation, Ki-67 immunohistochemistry was evaluated. Ki-67, a nuclear protein preferentially expressed during all active phases of the cell cycle (G1, S1 and G2) and mitosis, is absent in quiescent cells. The number of Ki-67 positive cells was low for both WT and *Thb*$^{-/-}$ hepatocytes (Fig.3d). Consistent with the results from the macroscopic observations, the labelling index from the 8-day exposure of mice to Wy showed a similar increase for both WT and *Thb*$^{-/-}$ hepatocytes (Fig. 3d) indicating that ThB was probably dispensable for cell proliferation in liver.

4.4. *Thb*$^{-/-}$ mice display regular peroxisome biogenesis and proliferation in liver

To assess for possible defects in peroxisomal assembly in *Thb*$^{-/-}$ mice, we performed microscopic studies of liver sections. At light microscopy level, these studies revealed a distinct pattern of numerous, DAB-reactive granules in the hepatocyte cytoplasm of WT mice, with normal peroxisome distribution (Fig. 4a). Similar peroxisome numbers and distribution were observed in *Thb*$^{-/-}$ hepatocytes, suggesting that ThB was dispensable for peroxisome biogenesis and proliferation in normal conditions (Fig. 4c). These results are coherent with similar gene expression of critical peroxins (such as Pex3p, Pex13p and Pex16p) in both WT and *Thb*$^{-/-}$ mice, indicating that ThB is dispensable for peroxisome biogenesis (supplemental Table 1). Wy-treatment caused massive peroxisome proliferation in both WT and *Thb*$^{-/-}$ hepatocytes (Fig. 4b, 4d). This result is consistent with the increased mRNA levels of the PPARα target gene *Pex11α* observed in both WT and *Thb*$^{-/-}$ mice (Fig. 4e). Taken together, these data indicate that ThB is dispensable for hepatic peroxisome proliferation induced by Wy.

Electron microscopy (EM) examination revealed that the liver peroxisomes were more elongated and slightly more numerous in *Thb*$^{-/-}$ mice than in WT mice (Fig. 4f, 4h). These data suggest that *Thb* deletion does not cause the massive spontaneous peroxisome proliferation that has been observed in the livers of mice deficient for *Acox1* [8]. As expected, after Wy-treatment, pronounced peroxisome proliferation was observed in both WT mice and *Thb*$^{-/-}$ mice.

4.5. *Thb* deletion blunts Wy-mediated upregulation of genes encoding for cholesterol biosynthesis enzymes

In order to ascertain whether some metabolic steps are affected by *Thb* deletion, detailed analysis of the microarray data was performed. In agreement with published data, Wy increased the expression of several genes involved in *de novo* cholesterol biosynthesis (Fig. 5 and supplemental Table 1) [44, 45]. However, this effect was significantly blunted in *Thb*$^{-/-}$ mice, as shown by RT-qPCR (Fig. 6). Similar data were collected for fenofibrate (Fig. 7). These data suggest that ThB may be involved in hepatic cholesterol homeostasis *via* indirect regulation of the expression of genes encoding for cholesterol biosynthesis enzymes.

4.6. Reduced content of cholesterol biosynthesis enzymes in the liver of Wy-treated *Thb*$^{-/-}$ mice is not secondary to reduced maturation of SREBP-2.

Since the rate-controlling step in cholesterol biosynthesis is catalyzed by HMG-CoA reductase, we checked whether the induction of *Hmg-CoA reductase* mRNA by Wy was translated at the protein level. In coherence with the mRNA data, Wy increased HMG-CoA reductase protein content in WT mice, but not in *Thb*$^{-/-}$ mice (Fig. 8a). A similar pattern was observed for two enzymes found in peroxisomes, phosphomevalonate kinase (Pmvk) and mevalonate kinase (Mvk), (Fig. 8a). However, the p*mvk* mRNA levels did not reflect the increase in Pmvk at the enzyme level. Therefore, we cannot completely rule out some post-translational modifications by intermediates of the cholesterol and nonsterol isoprene biosynthetic pathways, as previously shown for Mvk [46]. In coherence with an intact PPARα signalling cascade in *Thb*$^{-/-}$ mice, the nuclear PPARα content was not affected by *Thb* deletion or by the Wy-treatment (Fig. 8b).

Since genes encoding for cholesterol biosynthesis enzymes are under the direct control of the transcription factor SREBP-2, the *Srebp-2* mRNA level was quantified in liver samples of fibrate-treated or mock-treated WT and *Thb*$^{-/-}$ mice. No significant effects of Wy ($p=0.792$), fenofibrate ($p=0.083$) or *Thb* deletion ($p=0.71$) on hepatic *Srebp-2* mRNA were observed (Fig. 8c). Whatever the genotype and pharmacological activation, the mature nuclear form of SREBP-2 remained constant (Fig. 8c). These data suggest that the decrease in induction of cholesterol synthesis gene

expression in fibrate-treated *Thb*$^{-/-}$ mice is probably not the consequence of defects in the maturation process of SREBP-2.

4.7. The rate of in vivo cholesterol synthesis is reduced by Wy-treatment in both WT mice and *Thb*$^{-/-}$ mice.

To investigate if the impact of *Thb* deletion on cholesterol synthesizing genes expression in the liver results in an altered rate of cholesterol synthesis, the plasma lathosterol (5α-cholest-7-en-3β-ol) to cholesterol ratio was determined. This ratio correlates well with the cholesterol balance and has been used as an index of cholesterol biosynthesis [47, 48]. As reported in the literature, the lathosterol/cholesterol ratio measured in the liver and in plasma was significantly reduced by Wy-treatment (Wy; p=0.007) and fenofibrate-treatment (FF; p=0.042) in WT mice and in *Thb*$^{-/-}$ mice (Fig. 9a and 9c). In the liver, however, the steady-state hepatic cholesterol (total and free) content remained stable after Wy-treatment in both WT mice and *Thb*$^{-/-}$ mice, suggesting potential compensatory mechanisms such as a decrease in catabolism of cholesterol to bile acids and/or a decrease in its excretion in the stool (Fig. 9b and 9d).

5. Discussion

We recently reported on the hepatic enrichment of (n-7) and (n-9) mono-unsaturated fatty acids (MUFAs) in the livers of Wy-treated *Thb*$^{-/-}$ mice [49]. Here, using radiolabelled (1-^{14}C) palmitate, we show that peroxisomal fatty acid oxidation is not impaired by *Thb* deletion in the livers of mock-treated mice. This new finding suggests that ThA and/or SCPx/SCP2 thiolase could replace ThB in the absence of pharmacological stress.

After Wy-treatment, there was weaker induction of peroxisomal fatty acid oxidation in *Thb*$^{-/-}$ mice, indicating that ThA and/or SCPx/SCP2 thiolase cannot fully compensate for the lack of ThB under conditions of metabolic stress. The role of ThB in the liver becomes crucial for peroxisomal fatty

acid oxidation when this function is activated. Even though ThA and ThB share almost complete amino acid similarity (96% identity), they do not necessarily share the same natural substrates and their relative affinity for their substrates could be different [2].

It has previously been reported that the livers of *Pex2*- or *Pex5*-deficient mice are devoid of functional peroxisomes [50, 51]. Elsewhere, fibroblasts derived from patients with ACOX1 or MFP2 deficiency have been shown to exhibit a fivefold reduction in peroxisome abundance [52]. However, in some peroxisomal-disorder patients, peroxisome abundance was normal but their form was elongated [53, 54]. Here, we report that *Thb*$^{-/-}$ mice have slightly elongated peroxisomes, but the mechanism underlying this potentially interesting phenotype remains to be investigated.

Mice deficient for peroxisomal oxidative enzymes have fewer peroxisomes, supporting the hypothesis that peroxisomal β-oxidation could partly control peroxisome abundance. Given that reduced peroxisomal β-oxidation was observed in Wy-treated *Thb*$^{-/-}$ mice, we investigated the function of ThB in this cellular process. Peroxisome abundance was shown to be related to the presence or absence of Wy-treatment and not to genotype. Wy-treated *Thb*$^{-/-}$ and WT mice both had more peroxisomes than the mock-treated mice, indicating that the role of ThB in peroxisome proliferation is minimal. Pex7-deficient mice have a disrupted peroxisomal receptor for ThB import, but they nevertheless display normal peroxisome assembly, which confirms that peroxisomal ThB is dispensable for peroxisome biogenesis [55]. One possible hypothesis is that ThA and/or SCPX/SCP2 could compensate for the absence of ThB. However, similar *Scpx/Scp2* mRNA levels were found in WT and *Thb*$^{-/-}$ mice, making the SCPX/SCP2 hypothesis unlikely. Furthermore, SCPX/SCP2-deficient mice had more peroxisomes in their livers, indicating that SCPX/SCP2 could impede peroxisome proliferation [6]. Elevated *Tha* mRNA levels in Wy-treated *Thb*$^{-/-}$ mice could reflect a response to the previously reported hepatic overload of (n-7) and (n-9) MUFAs (Fig. 1) [49]. As the substrates and properties of ThA and ThB have still not been completely explored, it is impossible to rule out a mechanism where ThA compensates for the absence of ThB, similar to the compensation observed between MFP-1 and MFP-2 in mice

deficient for these genes [56], (and reviewed in Ref. [5]), [57]. Thus, the generation of *Tha*$^{-/-}$ mice would be a positive step in exploring the role of ThA in peroxisome biogenesis, proliferation and function. It could also help to clarify the respective contribution of ThA and ThB to various substrates [56].

In contrast to *Pex5*$^{-/-}$ mice, which show a twofold increase in mitochondrial palmitate β-oxidation, mitochondrial palmitate β-oxidation remains unchanged in *Thb*$^{-/-}$ mice [58]. Furthermore, since *Thb* deletion appears to have no effect on the structure of the mitochondria as revealed by electron microscopy and on the activity of mitochondrial marker enzymes, we conclude that the biology of the mitochondrion is not dependent on ThB.

Previous studies have described an incomplete cholesterol biosynthesis pathway in peroxisomes, with conversion of the peroxisomal acetyl-CoA pool to HMG-CoA. The peroxisomal acetyl-CoA pool produced by β-oxidation represents less than 10% of the total acetyl-CoA in the liver [59] and is channelled preferentially to cholesterol biosynthesis [60-63]. Cholesterol biosynthesis followed the same pattern in both *Thb*$^{-/-}$ and WT mice. As the total and free cholesterol content in the liver was also similar in both *Thb*$^{-/-}$ and WT mice, ThB probably has a limited functional role in this pathway, but compensation by ThA and/or SCPx/SCP2 cannot be ruled out.

It is worth recalling that our expression data are in coherence with the existing literature, showing the induction of some genes encoding for cholesterol biosynthesis enzymes after Wy-treatment in the livers of WT mice, but intriguingly not in those of *Thb*$^{-/-}$ mice [44, 45]. However, the increase in most mRNAs and proteins encoding for cholesterol biosynthesis after Wy-treatment in WT mice was not accompanied by an increase in *de novo* cholesterol biosynthesis, as shown by the plasma lathosterol/cholesterol ratio, a surrogate plasma marker for endogenous cholesterol biosynthesis downstream from lanosterol [47]. These data are in line with various studies showing that fibrate-treatment in WT mice does not stimulate hepatic production of cholesterol but rather decreases it [45]. Given that well-established PPARα target genes are equally upregulated in Wy-treated WT and *Thb*$^{-/-}$ mice, why is it that SREBP-2 target genes (genes encoding for cholesterol biosynthesis

enzymes) do not follow the same pattern in Wy-treated WT and *Thb*$^{-/-}$ mice [49]? Recent studies have reported cross-talk between PPARα and SREBP-2 dependent gene-regulation in human hepatoma HepG2 cells, suggesting potential synergy between the PPARα and SREBP-2 pathways in humans [64, 65]. It is possible that the SREBP-2 and perhaps even the SREBP-1 signalling cascades may be compromised in Wy-treated *Thb*$^{-/-}$ mice. However, many animal and cellular studies exploring the level of expression of SREBP-2 and SREBP-1 have shown that, while SREBP-2 is a relatively selective activator of cholesterol biosynthesis, SREBP-1 controls fatty acid biosynthesis (reviewed in Refs. [66-68]). The mRNAs for several cholesterol biosynthesis enzymes have been found to increase in transgenic mice expressing a dominant positive NH2-terminal fragment of SREBP-la [69]. One possible hypothesis is that a decrease in SREBP-1 could cause a decrease in the Wy-induction of genes encoding for cholesterol biosynthesis enzymes in *Thb*$^{-/-}$ mice. However, we consider this explanation very unlikely, as the maturation of SREBP-2 and SREBP-1 is unaltered in *Thb*$^{-/-}$ mice (this manuscript and Ref. [49]). In further support of this notion, the mRNA levels of the lipogenic genes *Accα* and *Fas*, two SREBP-1 targets, were more elevated in Wy-treated *Thb*$^{-/-}$ mice than in Wy-treated WT mice, suggesting that the SREBP-1 pathway was not compromised [49]. No difference in the mRNA level or the mature active form of the protein was observed for SREBP-2 in WT and *Thb*$^{-/-}$ mice, with or without Wy-treatment. The activity of nuclear SREBP-2 is regulated by post-translational modifications [70]. For example, insulin-like growth factor 1 (IGF-1) induces phosphorylation of SREBP-2, facilitating SREBP-2 transcriptional activity and thereby the expression of its target genes [70]. *Thb*$^{-/-}$ mice are smaller than WT mice and display a drastic reduction in liver *Igf-1* mRNA and circulating levels (unpublished data). A plausible hypothesis that should not be dismissed is that reduced IGF-1-mediated phosphorylation of SREBP-2 could ultimately lead to reduced transcriptional activity of SREBP-2 in Wy-treated *Thb*$^{-/-}$ mice.

Almost all the biological effects of Wy on gene expression have been shown to be mediated by the nuclear receptor PPARα [31]. The Wy-induction of genes encoding for cholesterol biosynthesis enzymes has been shown to be dependent on PPARα [44, 45, 71]. Based on these statements, we may speculate that the PPARα signalling cascade may be altered by *Thb* deletion, explaining at least in part the non-induction of genes encoding for cholesterol biosynthesis enzymes in Wy-treated *Thb*$^{-/-}$ mice. However, the magnitude of Wy- or fibrate-induction in almost all typical hepatic PPARα target genes appears to remain at least the same in *Thb*$^{-/-}$ mice, arguing against this possibility (Fig. 1d and supplemental Fig. 2a and 2b) [49]. Significantly, van der Meer *et al* found PPARα binding to the human promoter of the SREBP target genes *Hmgcs1, Hmgcr, Fdft1 and Sc4mol,* confirming cross-talk between PPARα and SREBP [64]. In further support of this idea, Leuenberger *et al* also reported the physical binding of PPARα to the promoter of the *Hmgcs1*, *Hmgcr*, *Mvk* and *Pmvk* genes in Wy-treated mice [65]. Together, these results indicate that activated PPARα could perhaps directly but unexpectedly control hepatic cholesterol biosynthesis. In order to link PPARα unequivocally to the impaired Wy-induction of genes encoding for cholesterol biosynthesis enzymes, it would be necessary to establish *Pparα*$^{-/-}$ x *Thb*$^{-/-}$ mice.

Another key nuclear receptor for cholesterol biosynthesis is the oxysterol receptor Liver X Receptor α (LXRα), which is regulated at the transcriptional level by PPARα [72, 73]. By silencing the expression of the two genes *Cyp51* and *Fdft1* encoding key cholesterologenic enzymes *via* a negative DNA response element, LXRα counteracts the effects of SREBP-2. However, LXRα is probably not involved in the impaired Wy-induction of *Cyp51* and *Fdft1* genes in *Thb*$^{-/-}$ mice because the expression of *Lxrα* and its target genes was unaltered in Wy-treated *Thb*$^{-/-}$ mice (data not shown and [49]).

In our previous comparative analysis of liver and plasma fatty acid composition, we found a reduction in DHA (Docosahexaenoic acid, C22:6(n-3), a potent natural activator of PPARα *in vivo*) in Wy-treated *Thb*$^{-/-}$ mice, [31, 49]. There was also a reduction in hepatic arachidonic acid

(C20:4(n-6)), a natural agonist for the Retinoid X Receptor, in Wy-treated *Thb*$^{-/-}$ mice [49, 74]. Furthermore, recent data have also indicated that C16:1(n-7) decreases activation of the PPARα target gene in the liver [75]. The amount of C16:1(n-7) is significantly increased in the livers of Wy-treated *Thb*$^{-/-}$ mice. Changes in the availability of this metabolite in *Thb*$^{-/-}$ mice may therefore decrease the Wy-induction of cholesterologenic genes by selectively modulating receptor-coregulator interactions.

Finally, it should be emphasized that Wy-treated *Thb*$^{-/-}$ mice displayed enrichment of some (n-7) and (n-9) MUFAs in the liver, as the probable consequence of higher Stearoyl-CoA Desaturase-1 (SCD1) activity [49]. Recent findings indicate that changes in the hepatic fatty acid composition of the products of SCD1 modulate free cholesterol biosynthesis through a mechanism that implies endoplasmic reticulum (ER) stress [76, 77]. While we cannot completely rule out a role for ER stress in the dysregulation of SREBP-2 target genes by Wy in *Thb*$^{-/-}$ mice, this explanation appears very unlikely because deleting the *Thb* gene in mice did not affect the expression pattern of the main genes involved in the emergence of ER stress, as revealed by DNA arrays (data not shown).

To conclude, our data suggest that ThB plays a minor role in peroxisome biogenesis and proliferation in the liver. The present work also suggests that under certain conditions of metabolic stress, ThB may contribute to the indirect regulation by activated PPARα of SREBP-2 target gene expression. Like other studies on MFP-2 and Pex2p, our data strengthen the notion that defects in peroxisomal enzymes impact on the mRNA levels of genes encoding for cholesterol biosynthesis enzymes in the liver [14, 78]. There may possibly be molecular and biochemical mechanisms to explain our observations and these avenues should therefore be explored by direct experimentation in the future.

Acknowledgments: This work was supported by grants from the European Union project "Peroxisomes" LSHG-CT-2004-512018, the Regional Council of Burgundy and the INSERM U866 center (Dijon). G.C. was supported by a French Ministry of Research and Technology Ph.D. fellowship and M.F. by the Italian "Ministero della Ricerca Scientifica e Tecnologica".

We thank staff members from the Centre de Zootechnie (Dijon, France) for their help in mice housing and breeding, Jacques Kaminski for laboratory analyses and Dr Wim Kulik (Academic Medical Center, University of Amsterdam) for carrying out the measurement of mevalonate in liver homogenate samples. We are grateful to Amandine Bataille (Plateau technique d'imagerie cellulaire CellImaP, IFR 100 Santé-STIC, Dijon) for her expertise in performing histological studies. We are also indebted to Mechteld Grootte-Bromhaar for performing the micro-array experiment and to Drs. Philip J. de Groot and Guido J.E.J. Hooiveld for their valuable contribution to the analysis of the micro-array data. The authors are also indebted to Ms Carmela Chateau-Smith for reviewing the English version of the manuscript.

Abbreviations: ThB: peroxisomal 3-ketoacyl-CoA thiolase B; ThA: peroxisomal 3-ketoacyl-CoA thiolase A; ACOX1 (for human protein) or Acox1 (for mouse protein): peroxisomal acyl-CoA oxidase-I; CPT-1α: carnitine palmitoyltransferase-1alpha; DAB: DiAminoBenzidine; PPARα: Peroxisome Proliferator-Activated Receptor alpha; LCFAs: Long-Chain Fatty Acids; VLCFAs: Very-Long-Chain Fatty Acids; MUFAs: Mono-Unsaturated Fatty Acids; Wy: Wy14,643; FF: Fenofibrate.

References

[1] R.J. Wanders, S. Ferdinandusse, P. Brites, S. Kemp, Peroxisomes, lipid metabolism and lipotoxicity, Biochim. Biophys. Acta 1801 (2010) 272-280.

[2] G. Chevillard, M.C. Clemencet, P. Etienne, P. Martin, T. Pineau, N. Latruffe, V. Nicolas-Frances, Molecular cloning, gene structure and expression profile of two mouse peroxisomal 3-ketoacyl-CoA thiolase genes, BMC Biochem. 5 (2004) 3.

[3] M. Hijikata, J.K. Wen, T. Osumi, T. Hashimoto, Rat peroxisomal 3-ketoacyl-CoA thiolase gene. Occurrence of two closely related but differentially regulated genes, J. Biol. Chem. 265 (1990) 4600-4606.

[4] A. Bout, M.M. Franse, J. Collins, L. Blonden, J.M. Tager, R. Benne, Characterization of the gene encoding human peroxisomal 3-oxoacyl-CoA thiolase (ACAA). No large DNA rearrangement in a thiolase-deficient patient, Biochim. Biophys. Acta 1090 (1991) 43-51.

[5] Y. Poirier, V.D. Antonenkov, T. Glumoff, J.K. Hiltunen, Peroxisomal beta-oxidation--a metabolic pathway with multiple functions, Biochim Biophys Acta 1763 (2006) 1413-1426.
[6] U. Seedorf, M. Raabe, P. Ellinghaus, F. Kannenberg, M. Fobker, T. Engel, S. Denis, F. Wouters, K.W. Wirtz, R.J. Wanders, N. Maeda, G. Assmann, Defective peroxisomal catabolism of branched fatty acyl coenzyme A in mice lacking the sterol carrier protein-2/sterol carrier protein-x gene function, Genes Dev. 12 (1998) 1189-1201.
[7] C.Y. Fan, J. Pan, R. Chu, D. Lee, K.D. Kluckman, N. Usuda, I. Singh, A.V. Yeldandi, M.S. Rao, N. Maeda, J.K. Reddy, Hepatocellular and hepatic peroxisomal alterations in mice with a disrupted peroxisomal fatty acyl-coenzyme A oxidase gene, J. Biol. Chem. 271 (1996) 24698-24710.
[8] C.Y. Fan, J. Pan, N. Usuda, A.V. Yeldandi, M.S. Rao, J.K. Reddy, Steatohepatitis, spontaneous peroxisome proliferation and liver tumors in mice lacking peroxisomal fatty acyl-CoA oxidase. Implications for peroxisome proliferator-activated receptor alpha natural ligand metabolism, J. Biol. Chem. 273 (1998) 15639-15645.
[9] S. Ferdinandusse, S. Denis, E.M. Hogenhout, J. Koster, C.W. van Roermund, I.J. L, A.B. Moser, R.J. Wanders, H.R. Waterham, Clinical, biochemical, and mutational spectrum of peroxisomal acyl-coenzyme A oxidase deficiency, Hum. Mutat. 28 (2007) 904-912.
[10] D. Oaxaca-Castillo, P. Andreoletti, A. Vluggens, S. Yu, P.P. van Veldhoven, J.K. Reddy, M. Cherkaoui-Malki, Biochemical characterization of two functional human liver acyl-CoA oxidase isoforms 1a and 1b encoded by a single gene, Biochem. Biophys. Res. Commun. 360 (2007) 314-319.
[11] A. Vluggens, P. Andreoletti, N. Viswakarma, Y. Jia, K. Matsumoto, W. Kulik, M. Khan, J. Huang, D. Guo, S. Yu, J. Sarkar, I. Singh, M.S. Rao, R.J. Wanders, J.K. Reddy, M. Cherkaoui-Malki, Functional significance of the two ACOX1 isoforms and their crosstalks with PPARalpha and RXRalpha, Lab. Invest. 90 696-708.
[12] M. Baes, S. Huyghe, P. Carmeliet, P.E. Declercq, D. Collen, G.P. Mannaerts, P.P. Van Veldhoven, Inactivation of the peroxisomal multifunctional protein-2 in mice impedes the degradation of not only 2-methyl-branched fatty acids and bile acid intermediates but also of very long chain fatty acids, J. Biol. Chem. 275 (2000) 16329-16336.
[13] C. Qi, Y. Zhu, J. Pan, N. Usuda, N. Maeda, A.V. Yeldandi, M.S. Rao, T. Hashimoto, J.K. Reddy, Absence of spontaneous peroxisome proliferation in enoyl-CoA Hydratase/L-3-hydroxyacyl-CoA dehydrogenase-deficient mouse liver. Further support for the role of fatty acyl CoA oxidase in PPARalpha ligand metabolism, J. Biol. Chem. 274 (1999) 15775-15780.
[14] K. Martens, E. Ver Loren van Themaat, M.F. van Batenburg, M. Heinaniemi, S. Huyghe, P. Van Hummelen, C. Carlberg, P.P. Van Veldhoven, A. Van Kampen, M. Baes, Coordinate induction of PPARalpha and SREBP2 in multifunctional protein 2 deficient mice, Biochim. Biophys. Acta (2008).
[15] S. Ferdinandusse, E.G. van Grunsven, W. Oostheim, S. Denis, E.M. Hogenhout, I.J. L, C.W. van Roermund, H.R. Waterham, S. Goldfischer, R.J. Wanders, Reinvestigation of peroxisomal 3-ketoacyl-CoA thiolase deficiency: identification of the true defect at the level of d-bifunctional protein, Am. J. Hum. Genet. 70 (2002) 1589-1593.
[16] A.W. Schram, S. Goldfischer, C.W. van Roermund, E.M. Brouwer-Kelder, J. Collins, T. Hashimoto, H.S. Heymans, H. van den Bosch, R.B. Schutgens, J.M. Tager, et al., Human peroxisomal 3-oxoacyl-coenzyme A thiolase deficiency, Proc. Natl. Acad. Sci. U S A 84 (1987) 2494-2496.
[17] G. Chevillard, M.C. Clemencet, N. Latruffe, V. Nicolas-Frances, Targeted disruption of the peroxisomal thiolase B gene in mouse: a new model to study disorders related to peroxisomal lipid metabolism, Biochimie 86 (2004) 849-856.
[18] J.K. Reddy, T.P. Krishnakantha, Hepatic peroxisome proliferation: induction by two novel compounds structurally unrelated to clofibrate, Science 190 (1975) 787-789.
[19] S.S. Lee, T. Pineau, J. Drago, E.J. Lee, J.W. Owens, D.L. Kroetz, P.M. Fernandez-Salguero, H. Westphal, F.J. Gonzalez, Targeted disruption of the alpha isoform of the

peroxisome proliferator-activated receptor gene in mice results in abolishment of the pleiotropic effects of peroxisome proliferators, Mol. Cell. Biol. 15 (1995) 3012-3022.
[20] I. Issemann, S. Green, Activation of a member of the steroid hormone receptor superfamily by peroxisome proliferators, Nature 347 (1990) 645-650.
[21] P.R. Devchand, H. Keller, J.M. Peters, M. Vazquez, F.J. Gonzalez, W. Wahli, The PPARalpha-leukotriene B4 pathway to inflammation control, Nature 384 (1996) 39-43.
[22] P. Escher, O. Braissant, S. Basu-Modak, L. Michalik, W. Wahli, B. Desvergne, Rat PPARs: quantitative analysis in adult rat tissues and regulation in fasting and refeeding, Endocrinology 142 (2001) 4195-4202.
[23] S. Mandard, M. Muller, S. Kersten, Peroxisome proliferator-activated receptor alpha target genes, Cell. Mol. Life Sci. 61 (2004) 393-416.
[24] F. Hansmannel, M.C. Clemencet, C. Le Jossic-Corcos, T. Osumi, N. Latruffe, V. Nicolas-Frances, Functional characterization of a peroxisome proliferator response-element located in the intron 3 of rat peroxisomal thiolase B gene, Biochem. Biophys. Res. Commun. 311 (2003) 149-155.
[25] V. Nicolas-Frances, V.K. Dasari, E. Abruzzi, T. Osumi, N. Latruffe, The peroxisome proliferator response element (PPRE) present at positions -681/-669 in the rat liver 3-ketoacyl-CoA thiolase B gene functionally interacts differently with PPARalpha and HNF-4, Biochem. Biophys. Res. Commun. 269 (2000) 347-351.
[26] B. Desvergne, W. Wahli, Peroxisome proliferator-activated receptors: nuclear control of metabolism, Endocr. Rev. 20 (1999) 649-688.
[27] F.J. Gonzalez, Y.M. Shah, PPARalpha: mechanism of species differences and hepatocarcinogenesis of peroxisome proliferators, Toxicology 246 (2008) 2-8.
[28] R. Genolet, W. Wahli, L. Michalik, PPARs as drug targets to modulate inflammatory responses? Curr. Drug Targets Inflamm. Allergy 3 (2004) 361-375.
[29] R. Stienstra, S. Mandard, N.S. Tan, W. Wahli, C. Trautwein, T.A. Richardson, E. Lichtenauer-Kaligis, S. Kersten, M. Muller, The Interleukin-1 receptor antagonist is a direct target gene of PPARalpha in liver, J. Hepatol. 46 (2007) 869-877.
[30] M. Cherkaoui-Malki, K. Meyer, W.Q. Cao, N. Latruffe, A.V. Yeldandi, M.S. Rao, C.A. Bradfield, J.K. Reddy, Identification of novel peroxisome proliferator-activated receptor alpha (PPARalpha) target genes in mouse liver using cDNA microarray analysis, Gene Expr. 9 (2001) 291-304.
[31] L.M. Sanderson, P.J. de Groot, G.J. Hooiveld, A. Koppen, E. Kalkhoven, M. Muller, S. Kersten, Effect of synthetic dietary triglycerides: a novel research paradigm for nutrigenomics, PLoS One 3 (2008) e1681.
[32] Z.Y. Du, L. Demizieux, P. Degrace, J. Gresti, B. Moindrot, Y.J. Liu, L.X. Tian, J.M. Cao, P. Clouet, Alteration of 20:5n-3 and 22:6n-3 fat contents and liver peroxisomal activities in fenofibrate-treated rainbow trout, Lipids 39 (2004) 849-855.
[33] P. Degrace, L. Demizieux, J. Gresti, J.M. Chardigny, J.L. Sebedio, P. Clouet, Hepatic steatosis is not due to impaired fatty acid oxidation capacities in C57BL/6J mice fed the conjugated trans-10,cis-12-isomer of linoleic acid, J. Nutr. 134 (2004) 861-867.
[34] H. Weissbach, T.E. Smith, J.W. Daly, B. Witkop, S. Udenfriend, A rapid spectrophotometric assay of mono-amine oxidase based on the rate of disappearance of kynuramine, J. Biol. Chem. 235 (1960) 1160-1163.
[35] J.B. Robinson, Jr., P.A. Srere, Organization of Krebs tricarboxylic acid cycle enzymes in mitochondria, J. Biol. Chem. 260 (1985) 10800-10805.
[36] M. Bronfman, N.C. Inestrosa, F. Leighton, Fatty acid oxidation by human liver peroxisomes, Biochem. Biophys. Res. Commun. 88 (1979) 1030-1036.
[37] F. Roels, B. De Prest, G. De Pestel, Liver and chorion cytochemistry, J. Inherit. Metab. Dis. 18 Suppl 1 (1995) 155-171.
[38] I. Kerckaert, D. De Craemer, G. Van Limbergen, Practical guide for morphometry of human peroxisomes on electron micrographs, J. Inherit. Metab. Dis. 18 Suppl 1 (1995) 172-180.

[39] S. Mandard, R. Stienstra, P. Escher, N.S. Tan, I. Kim, F.J. Gonzalez, W. Wahli, B. Desvergne, M. Muller, S. Kersten, Glycogen synthase 2 is a novel target gene of peroxisome proliferator-activated receptors, Cell. Mol. Life Sci. 64 (2007) 1145-1157.
[40] G. Denis, S. Mandard, C. Humblet, M. Verlaet, J. Boniver, D. Stehelin, M.P. Defresne, D. Regnier, Nuclear localization of a new c-cbl related protein, CARP 90, during in vivo thymic apoptosis in mice, Cell. Death Differ. 6 (1999) 689-697.
[41] S. Hogenboom, G.J. Romeijn, S.M. Houten, M. Baes, R.J. Wanders, H.R. Waterham, Absence of functional peroxisomes does not lead to deficiency of enzymes involved in cholesterol biosynthesis, J. Lipid. Res. 43 (2002) 90-98.
[42] S. Miyazawa, T. Osumi, T. Hashimoto, The presence of a new 3-oxoacyl-CoA thiolase in rat liver peroxisomes, Eur. J. Biochem. 103 (1980) 589-596.
[43] M. Baarine, K. Ragot, E.C. Genin, H. El Hajj, D. Trompier, P. Andreoletti, M.S. Ghandour, F. Menetrier, M. Cherkaoui-Malki, S. Savary, G. Lizard, Peroxisomal and mitochondrial status of two murine oligodendrocytic cell lines (158N, 158JP): potential models for the study of peroxisomal disorders associated with dysmyelination processes, J. Neurochem. 111 (2009) 119-131.
[44] C. Le Jossic-Corcos, S. Duclos, L.C. Ramirez, I. Zaghini, G. Chevillard, P. Martin, T. Pineau, P. Bournot, Effects of peroxisome proliferator-activated receptor alpha activation on pathways contributing to cholesterol homeostasis in rat hepatocytes, Biochim. Biophys. Acta 1683 (2004) 49-58.
[45] B.L. Knight, A. Hebbachi, D. Hauton, A.M. Brown, D. Wiggins, D.D. Patel, G.F. Gibbons, A role for PPARalpha in the control of SREBP activity and lipid synthesis in the liver, Biochem. J. 389 (2005) 413-421.
[46] D.D. Hinson, K.L. Chambliss, M.J. Toth, R.D. Tanaka, K.M. Gibson, Post-translational regulation of mevalonate kinase by intermediates of the cholesterol and nonsterol isoprene biosynthetic pathways, J Lipid Res 38 (1997) 2216-2223.
[47] H.J. Kempen, J.F. Glatz, J.A. Gevers Leuven, H.A. van der Voort, M.B. Katan, Serum lathosterol concentration is an indicator of whole-body cholesterol synthesis in humans, J. Lipid. Res. 29 (1988) 1149-1155.
[48] J.J. Hamilton, M. Phang, S.M. Innis, Elevation of plasma lathosterol, as an indicator of increased cholesterol synthesis, in preterm (23-32 weeks gestation) infants given Intralipid, Pediatr. Res. 31 (1992) 186-192.
[49] S. Arnauld, M. Fidaleo, M.C. Clemencet, G. Chevillard, A. Athias, J. Gresti, R.J. Wanders, N. Latruffe, V. Nicolas-Frances, S. Mandard, Modulation of the hepatic fatty acid pool in peroxisomal 3-ketoacyl-CoA thiolase B-null mice exposed to the selective PPARalpha agonist Wy14,643, Biochimie 91 (2009) 1376-1386.
[50] E. Baumgart, I. Vanhorebeek, M. Grabenbauer, M. Borgers, P.E. Declercq, H.D. Fahimi, M. Baes, Mitochondrial alterations caused by defective peroxisomal biogenesis in a mouse model for Zellweger syndrome (PEX5 knockout mouse), Am. J. Pathol. 159 (2001) 1477-1494.
[51] P.L. Faust, M.E. Hatten, Targeted deletion of the PEX2 peroxisome assembly gene in mice provides a model for Zellweger syndrome, a human neuronal migration disorder, J. Cell. Biol. 139 (1997) 1293-1305.
[52] M. Funato, N. Shimozawa, T. Nagase, Y. Takemoto, Y. Suzuki, Y. Imamura, T. Matsumoto, T. Tsukamoto, T. Kojidani, T. Osumi, T. Fukao, N. Kondo, Aberrant peroxisome morphology in peroxisomal beta-oxidation enzyme deficiencies, Brain Dev. 28 (2006) 287-292.
[53] M. Schrader, E. Baumgart, A. Volkl, H.D. Fahimi, Heterogeneity of peroxisomes in human hepatoblastoma cell line HepG2. Evidence of distinct subpopulations, Eur. J. Cell. Biol. 64 (1994) 281-294.
[54] F. Roels, M. Pauwels, B.T. Poll-The, J. Scotto, H. Ogier, P. Aubourg, J.M. Saudubray, Hepatic peroxisomes in adrenoleukodystrophy and related syndromes: cytochemical and morphometric data, Virchows Arch. A. Pathol. Anat. Histopathol. 413 (1988) 275-285.

[55] P. Brites, A.M. Motley, P. Gressens, P.A. Mooyer, I. Ploegaert, V. Everts, P. Evrard, P. Carmeliet, M. Dewerchin, L. Schoonjans, M. Duran, H.R. Waterham, R.J. Wanders, M. Baes, Impaired neuronal migration and endochondral ossification in Pex7 knockout mice: a model for rhizomelic chondrodysplasia punctata, Hum. Mol. Genet. 12 (2003) 2255-2267.
[56] V.D. Antonenkov, P.P. Van Veldhoven, E. Waelkens, G.P. Mannaerts, Comparison of the stability and substrate specificity of purified peroxisomal 3-oxoacyl-CoA thiolases A and B from rat liver, Biochim Biophys Acta 1437 (1999) 136-141.
[57] Y. Jia, C. Qi, Z. Zhang, T. Hashimoto, M.S. Rao, S. Huyghe, Y. Suzuki, P.P. Van Veldhoven, M. Baes, J.K. Reddy, Overexpression of peroxisome proliferator-activated receptor-alpha (PPARalpha)-regulated genes in liver in the absence of peroxisome proliferation in mice deficient in both L- and D-forms of enoyl-CoA hydratase/dehydrogenase enzymes of peroxisomal beta-oxidation system, J. Biol. Chem. 278 (2003) 47232-47239.
[58] R. Dirkx, E. Meyhi, S. Asselberghs, J. Reddy, M. Baes, P.P. Van Veldhoven, Beta-oxidation in hepatocyte cultures from mice with peroxisomal gene knockouts, Biochem. Biophys. Res. Commun. 357 (2007) 718-723.
[59] T. Kasumov, J.E. Adams, F. Bian, F. David, K.R. Thomas, K.A. Jobbins, P.E. Minkler, C.L. Hoppel, H. Brunengraber, Probing peroxisomal beta-oxidation and the labelling of acetyl-CoA proxies with [1-(13C)]octanoate and [3-(13C)]octanoate in the perfused rat liver, Biochem J 389 (2005) 397-401.
[60] N. Aboushadi, W.H. Engfelt, V.G. Paton, S.K. Krisans, Role of peroxisomes in isoprenoid biosynthesis, J. Histochem. Cytochem. 47 (1999) 1127-1132.
[61] W.J. Kovacs, K.N. Tape, J.E. Shackelford, X. Duan, T. Kasumov, J.K. Kelleher, H. Brunengraber, S.K. Krisans, Localization of the pre-squalene segment of the isoprenoid biosynthetic pathway in mammalian peroxisomes, Histochem. Cell Biol. 127 (2007) 273-290.
[62] I. Weinhofer, M. Kunze, H. Stangl, F.D. Porter, J. Berger, Peroxisomal cholesterol biosynthesis and Smith-Lemli-Opitz syndrome, Biochem Biophys Res Commun 345 (2006) 205-209.
[63] W.J. Kovacs, K.N. Tape, J.E. Shackelford, T.M. Wikander, M.J. Richards, S.J. Fliesler, S.K. Krisans, P.L. Faust, Peroxisome deficiency causes a complex phenotype because of hepatic SREBP/Insig dysregulation associated with endoplasmic reticulum stress, J Biol Chem 284 (2009) 7232-7245.
[64] D.L. van der Meer, T. Degenhardt, S. Vaisanen, P.J. de Groot, M. Heinaniemi, S.C. de Vries, M. Muller, C. Carlberg, S. Kersten, Profiling of promoter occupancy by PPAR{alpha} in human hepatoma cells via ChIP-chip analysis, Nucleic. Acids Res. (2010).
[65] N. Leuenberger, S. Pradervand, W. Wahli, Sumoylated PPARalpha mediates sex-specific gene repression and protects the liver from estrogen-induced toxicity in mice, J. Clin. Invest. 119 (2009) 3138-3148.
[66] J.D. Horton, J.L. Goldstein, M.S. Brown, SREBPs: activators of the complete program of cholesterol and fatty acid synthesis in the liver, J. Clin. Invest. 109 (2002) 1125-1131.
[67] J.D. Horton, I. Shimomura, Sterol regulatory element-binding proteins: activators of cholesterol and fatty acid biosynthesis, Curr. Opin. Lipidol. 10 (1999) 143-150.
[68] J.D. Horton, I. Shimomura, M.S. Brown, R.E. Hammer, J.L. Goldstein, H. Shimano, Activation of cholesterol synthesis in preference to fatty acid synthesis in liver and adipose tissue of transgenic mice overproducing sterol regulatory element-binding protein-2, J. Clin. Invest. 101 (1998) 2331-2339.
[69] H. Shimano, J.D. Horton, I. Shimomura, R.E. Hammer, M.S. Brown, J.L. Goldstein, Isoform 1c of sterol regulatory element binding protein is less active than isoform 1a in livers of transgenic mice and in cultured cells, J. Clin. Invest. 99 (1997) 846-854.
[70] M. Arito, T. Horiba, S. Hachimura, J. Inoue, R. Sato, Growth factor-induced phosphorylation of sterol regulatory element-binding proteins inhibits sumoylation, thereby stimulating the expression of their target genes, low density lipoprotein uptake, and lipid synthesis, J Biol Chem 283 (2008) 15224-15231.

[71] M. Rakhshandehroo, L.M. Sanderson, M. Matilainen, R. Stienstra, C. Carlberg, P.J. de Groot, M. Muller, S. Kersten, Comprehensive Analysis of PPARalpha-Dependent Regulation of Hepatic Lipid Metabolism by Expression Profiling, PPAR Res 2007 (2007) 26839.
[72] Y. Wang, P.M. Rogers, C. Su, G. Varga, K.R. Stayrook, T.P. Burris, Regulation of cholesterologenesis by the oxysterol receptor, LXRalpha, J. Biol. Chem. 283 (2008) 26332-26339.
[73] K.A. Tobin, H.H. Steineger, S. Alberti, O. Spydevold, J. Auwerx, J.A. Gustafsson, H.I. Nebb, Cross-talk between fatty acid and cholesterol metabolism mediated by liver X receptor-alpha, Mol. Endocrinol. 14 (2000) 741-752.
[74] J. Lengqvist, A. Mata De Urquiza, A.C. Bergman, T.M. Willson, J. Sjovall, T. Perlmann, W.J. Griffiths, Polyunsaturated fatty acids including docosahexaenoic and arachidonic acid bind to the retinoid X receptor alpha ligand-binding domain, Mol. Cell. Proteomics 3 (2004) 692-703.
[75] H. Cao, K. Gerhold, J.R. Mayers, M.M. Wiest, S.M. Watkins, G.S. Hotamisligil, Identification of a lipokine, a lipid hormone linking adipose tissue to systemic metabolism, Cell 134 (2008) 933-944.
[76] M.T. Flowers, M.P. Keller, Y. Choi, H. Lan, C. Kendziorski, J.M. Ntambi, A.D. Attie, Liver gene expression analysis reveals endoplasmic reticulum stress and metabolic dysfunction in SCD1-deficient mice fed a very low-fat diet, Physiol Genomics 33 (2008) 361-372.
[77] C.M. Paton, J.M. Ntambi, Loss of stearoyl-CoA desaturase activity leads to free cholesterol synthesis through increased Xbp-1 splicing, Am J Physiol Endocrinol Metab.
[78] W.J. Kovacs, J.E. Shackelford, K.N. Tape, M.J. Richards, P.L. Faust, S.J. Fliesler, S.K. Krisans, Disturbed cholesterol homeostasis in a peroxisome-deficient PEX2 knockout mouse model, Mol. Cell. Biol. 24 (2004) 1-13.

Figure 1. Peroxisomal β-oxidation of (1-^{14}C) palmitate is impaired in *Thb*$^{-/-}$ mice treated with Wy, a potent PPARα agonist.

WT and *Thb*$^{-/-}$ mice were treated with Wy (30mg/kg of body weight) for 8 days or left untreated. At the end of the pharmacological intervention, the animals were fasted (starting at 4 a.m) for 6 hours before sacrifice a) Liver RNA (5 animals were used for each condition) was isolated and RT-qPCR was performed. Gene expression levels from the animals receiving vehicle only were set at 1. *Thb*: peroxisomal 3-ketoacyl-CoA thiolase B ; *Tha*: peroxisomal 3-ketoacyl-CoA thiolase A b) Western blot analysis of PTL (anti-peroxisomal 3-ketoacyl-CoA thiolase A and B proteins) in liver protein extracts from five animals. β-actin was used as a loading control marker c) Liver RNA was isolated and RT-qPCR was performed (From 6 to 20 animals were used per condition). Gene expression levels from the animals receiving vehicle only were set at 1. *Acox 1*: peroxisomal Acyl-CoA oxidase 1; *Mfp-1*: Multifunctional protein 1; *Scpx/Scp2* thiolase: Sterol carrier protein x/2 thiolase; Values are expressed as mean ± SEM. See supplemental data, Table 2 for primer sequences. d)

Western blot analysis of Acox1 in liver protein extracts from five animals. β-actin was used as a loading control marker e) Peroxisomal (1-^{14}C) palmitate β-oxidation and f) NADH production were quantified *in vitro* using whole liver homogenates from WT and *Thb*$^{-/-}$ mice (n=3) Values are expressed as mean ± SEM. Statistically significant differences were calculated using a two-way ANOVA for genotype (G), Wy14,643 (Wy) and the interaction between the two parameters (I).

Figure 2. Mitochondrial β-oxidation of (1-^{14}C) palmitate is not compromised in *Thb*$^{-/-}$ mice treated with the potent PPARα agonist, Wy.

(a) Mitochondrial (1-^{14}C) palmitate β-oxidation in liver homogenates (b) Mitochondrial (1-^{14}C) palmitate β-oxidation in mitochondrial fractions. WT and *Thb*$^{-/-}$ mice were treated with Wy (30mg/kg of body weight) for 8 days, or left untreated. At the end of the pharmacological intervention, the animals were fasted (starting at 4 a.m) for 6 hours before sacrifice. Three animals were used per condition. Values are expressed as mean ± SEM. Statistically significant differences were calculated using a two-way ANOVA for genotype (G), Wy14,643 (Wy) and the interaction between the two parameters (I).

Figure 3. *Thb* Deletion did not prevent Wy-induced cell-size increase and cell proliferation rates.

(a) Hepato-somatic index of Wy-treated (30 mg/kg of body weight, 8 days) or mock-treated WT and *Thb*$^{-/-}$ mice. Five to ten animals were used per group. Error bars represent ± SEM. Statistically significant differences were calculated using a two-way ANOVA for genotype (G), Wy14,643 (Wy) and the interaction between the two parameters (I) (b) Mean cell number/field and cell surface in the liver of WT mice and *Thb*$^{-/-}$ mice (c) Hematoxylin and eosin staining of representative mouse liver sections showing increased hepatocyte size following Wy-treatment. Scale bar, 20 μm. (d) Immunohistochemical staining for Ki-67 in hepatocyte nuclei in liver sections from Wy-treated and mock-treated WT and *Thb*$^{-/-}$ mice. Scale bar, 20 μm.

Figure 4. *Thb* deletion did not prevent Wy-induced peroxisome proliferation.

(a-d) Immunohistochemical staining of peroxisomes in the liver. Light microscopy of semithin liver sections from 3-month-old mice after incubation with the alkaline DAB-medium to demonstrate catalase activity; arrows indicate some hepatocyte nuclei. (a) Liver from a WT mouse, showing a distinct granular staining pattern, reflecting normal peroxisome distribution (c) A similar staining pattern is found in the liver of a *Thb*$^{-/-}$ mouse (b and d) Peroxisome proliferation is prominent after Wy-treatment in WT and *Thb*$^{-/-}$ mice (e) Liver RNA was isolated and RT-qPCR was performed (n =6). Gene expression levels from the animals receiving vehicle only were set at 1. Statistically significant differences were calculated using a two-way ANOVA for genotype (G), Wy14,643 (Wy) and the interaction between the two parameters (I). Pex11α: Peroxisomal biogenesis factor 11α ; (f-i) Representative electron micrographs of mouse-liver sections without treatment (f,h) and after Wy-treatment (g,i). Note the presence of peroxisomes with a slightly elongated shape (see arrows) in h in contrast to the rounded shapes in f. Glycogen rosettes, specific for hepatic parenchyma were present in many cells. M: Mitochondria.

Figure 5: Heat map showing changes in expression of selected genes encoding for cholesterol biosynthesis enzymes in the liver as determined by microarray.

WT and *Thb*$^{-/-}$ mice were treated with Wy (30 mg/kg/day for 8 days) or left untreated, and all animals were fasted for 6h prior to sacrifice. Pooled liver RNA (n=5) was hybridized on Affymetrix GeneChip Mouse Genome 430A arrays. Expression levels were analyzed using Microarray Suite and Data Mining Tool software, as previously described [29]. The heat map was generated directly from the microarray data. The expression signals from the mock-treated WT animals were arbitrarily set at 1 and the scale represents fold-induction relative to mock-treated WT mice. The selected genes exceeded minimal threshold expression levels.

Figure 6: The hepatic expression of genes involved in *de novo* cholesterol biosynthesis is impaired in Wy-treated *Thb*$^{-/-}$ mice. WT (n=5) and *Thb*$^{-/-}$ (n=5) mice were treated with Wy (30mg/kg of body weight, 8 days), or left untreated. All animals were fasted for 6h prior to sacrifice. Liver RNA was isolated and RT-qPCR was performed. Gene expression levels from the animals receiving vehicle only were set at 1. *Hmgcs1* : cytosolic 3-hydroxy-3-methylglutaryl coenzyme A (HMG-CoA) synthase-1, *Hmgcr* : microsomal 3-hydroxy-3-methylglutaryl coenzyme A (HMG-CoA) reductase, *Mvk*: mevalonate kinase, *Pmvk*: phosphomevalonate kinase, mvd: mevalonate decarboxylase, *Fdps*: farnesyl diphosphate synthase, *Fdft1*: farnesyl-diphosphate farnesyltransferase-1, *Sqls*: squalene synthase, sqle: squalene epoxidase, *Lss*: lanosterol synthase, *Cyp51*: sterol 14 alpha-demethylase, *Nsdhl*: NAD(P) dependent steroid dehydrogenase-like, *Sc5d*: sterol-C5-desaturase, *Dhcr7*: 7-dehydrocholesterol reductase. Error bars represent ± SEM. Statistically significant differences were calculated using a two-way ANOVA for genotype (G), Wy14,643 (Wy) and the interaction between the two parameters (I). See supplemental data, Table 2 for primer sequences.

Figure 7: The hepatic expression of genes involved in *de novo* cholesterol biosynthesis is impaired in fenofibrate-treated *Thb*$^{-/-}$ mice.

WT (n=5) and *Thb*$^{-/-}$ (n=5) mice were previously treated with fenofibrate (100mg/kg of body weight) for 14 days, or left untreated. All animals were fasted for 6h prior to sacrifice. Liver RNA was isolated and RT-qPCR was performed. Gene expression levels from the animals receiving vehicle only were set at 1. *Hmgcs1* : cytosolic 3-hydroxy-3-methylglutaryl coenzyme A (HMG-CoA) synthase-1, *Hmgcr* : microsomal 3-hydroxy-3-methylglutaryl coenzyme A (HMG-CoA) reductase, *Mvk*: mevalonate kinase, *Pmvk*: phosphomevalonate kinase, *Mvd*: mevalonate decarboxylase, *Sqls*: squalene synthase, *Srebp1c*: sterol response element binding protein-1c, *Ppar*α : peroxisome proliferator-activated receptor alpha, FF: Fenofibrate. Statistically significant

differences were calculated using a two-way ANOVA for genotype (G), fenofibrate (FF) and the interaction between the two parameters (I). See supplemental data, Table 2 for primer sequences.

Figure 8: Expression of hepatic HMG-CoA reductase, Mvk and Pmvk proteins is reduced in Wy-treated *Thb*$^{-/-}$ mice (a) Pooled total liver cell lysates from Wy-treated or mock-treated WT and *Thb*$^{-/-}$ mice (30mg/kg of body weight, 8 days) and fasted for 6h prior to sacrifice. Analyses for mouse HMG-CoA reductase, Mvk and Pmvk protein content were conducted by Western blotting, using polyclonal antibodies. There were 5 animals per group except for the WT group (n=10). Molecular mass sizes are given in kDa. Quantification of bands relative to β-actin controls is given under each picture (b) Western blot analysis of PPARα was performed on nuclear extracts from the livers of five animals. Cellular lysates of COS-7 cells transfected with the expression vector pSG5 PPARα were used as a positive control. Histone H1 was used as a loading control marker (c) WT (n=5) and *Thb*$^{-/-}$ (n=5) mice were treated with Wy for 8 days or left untreated. All animals were fasted for 6h prior to sacrifice. Liver RNA was isolated and RT-qPCR was performed for *Srebp-2*. Statistically significant differences were calculated using a two-way ANOVA for genotype (G), Wy14,643 (Wy) and the interaction between the two parameters (I). Pooled nuclear extracts from mock-treated or Wy- or fenofibrate-treated WT and *Thb*$^{-/-}$ mice were analyzed by Western blotting for the mouse mature form of the transcription factor SREBP-2 (right part). Histone H1 or Tata-Binding Protein (TBP) were used for normalization of nuclear proteins. Wy: Wy14,643, FF: Fenofibrate.

Figure 9: *De novo* whole body cholesterol biosynthesis is equally reduced by activated PPARα in both WT mice and *Thb*$^{-/-}$ mice.

a) Plasma lathosterol/cholesterol ratio in mock-treated and Wy-treated WT and *Thb*$^{-/-}$ mice (n = 5 per condition) and fasted for 6h prior to sacrifice b) Total and free cholesterol in liver (n=5 to 10 mice per group) c) liver lathosterol/cholesterol ratio and d) total cholesterol in mock-treated and

fenofibrate-treated WT and *Thb*$^{-/-}$ mice and fasted for 6h prior to sacrifice (n = 4 per condition). Error bars represent ± SEM. Statistically significant differences were calculated using a two-way ANOVA for genotype (G), Wy14,643 (Wy) and the interaction between the two parameters (I).

Table 1. Mitochondrial marker enzyme activities in the liver are not affected by the deletion of *Thb* in mice. Carnitine Palmitoyl Transferase-1 alpha (CPT-Iα), monoamine oxidase, citrate synthase activities were measured in purified mitochondria. Wy: Wy14,643. Number of animals per group is indicated. Mice in the fed state were sacrificed at the beginning of the light cycle. For the fasting experiment, male mice were fasted for 24 hours starting at the onset of the light cycle. Statistically significant differences were calculated using a two-way ANOVA for genotype (G), Wy14,643 (Wy), fasting (F) and interaction between the two parameters (I).

Supplemental Figure 1.

Similar levels of typical PPARα target gene induction were observed in the livers of WT and *Thb*$^{-/-}$ mice treated with two different PPARα agonists. a) mock-treated and Wy-treated (30mg/kg of body weight for 8 days) WT and *Thb*$^{-/-}$ mice and fasted for 6h prior to sacrifice b) mock-treated and fenofibrate-treated (100mg/kg of body weight for 14 days) WT and *Thb*$^{-/-}$ mice and fasted for 6h prior to sacrifice. Liver RNA was isolated and RT-qPCR was performed. Five to eight animals were used for each condition. Gene expression levels from the animals receiving vehicle only were set at 1. See supplemental Table 2 for primer sequences. FF: Fenofibrate. Wy: Wy14,643. *Acot3*: Acyl-CoA thioesterase 3; *Pdk4*: Pyruvate dehydrogenase kinase-4; *Fat/Cd36*: Fatty acid translocase; *a-Fabp*: adipose-Fatty acid binding protein (also known as aP2); *Thb*: Thiolase B; *Cyp4a10*: Cytochrome p450A10; *Lpl*: Lipoprotein Lipase; *Fatp-1*: Fatty acid transport-1.

Supplemental Table 1.

Micro-array analysis was performed on pooled liver (n=5) mRNA comparing the gene expression signals induced by the deletion of *Thb* and by pharmacological intervention (Wy, 30 mg/kg of body weight/ 8 days). Column C to F: Expression in mock-treated WT mice was arbitrarily set at 1. Changes in gene expression are expressed as fold-changes in comparison with mock-treated WT mice, receiving vehicle only.

Supplemental Table 2.

Primer sequences used for Real-Time Quantitative PCR.

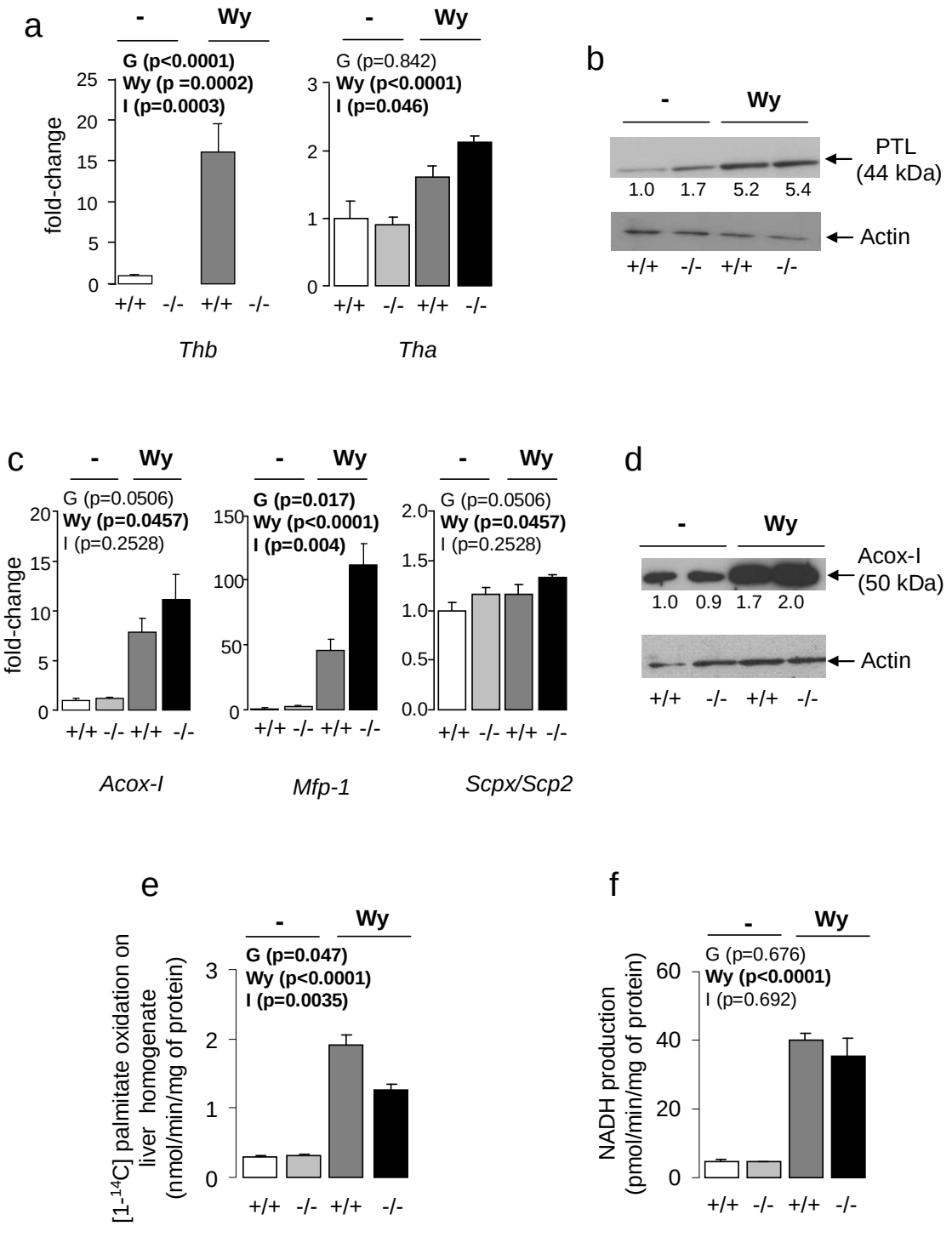

Fidaleo *et al*., Figure 1

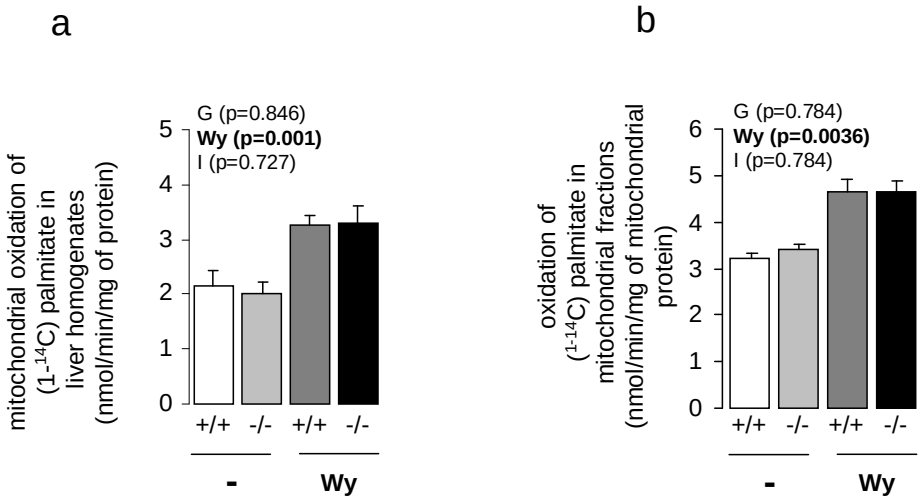

Fidaleo *et al*., Figure 2

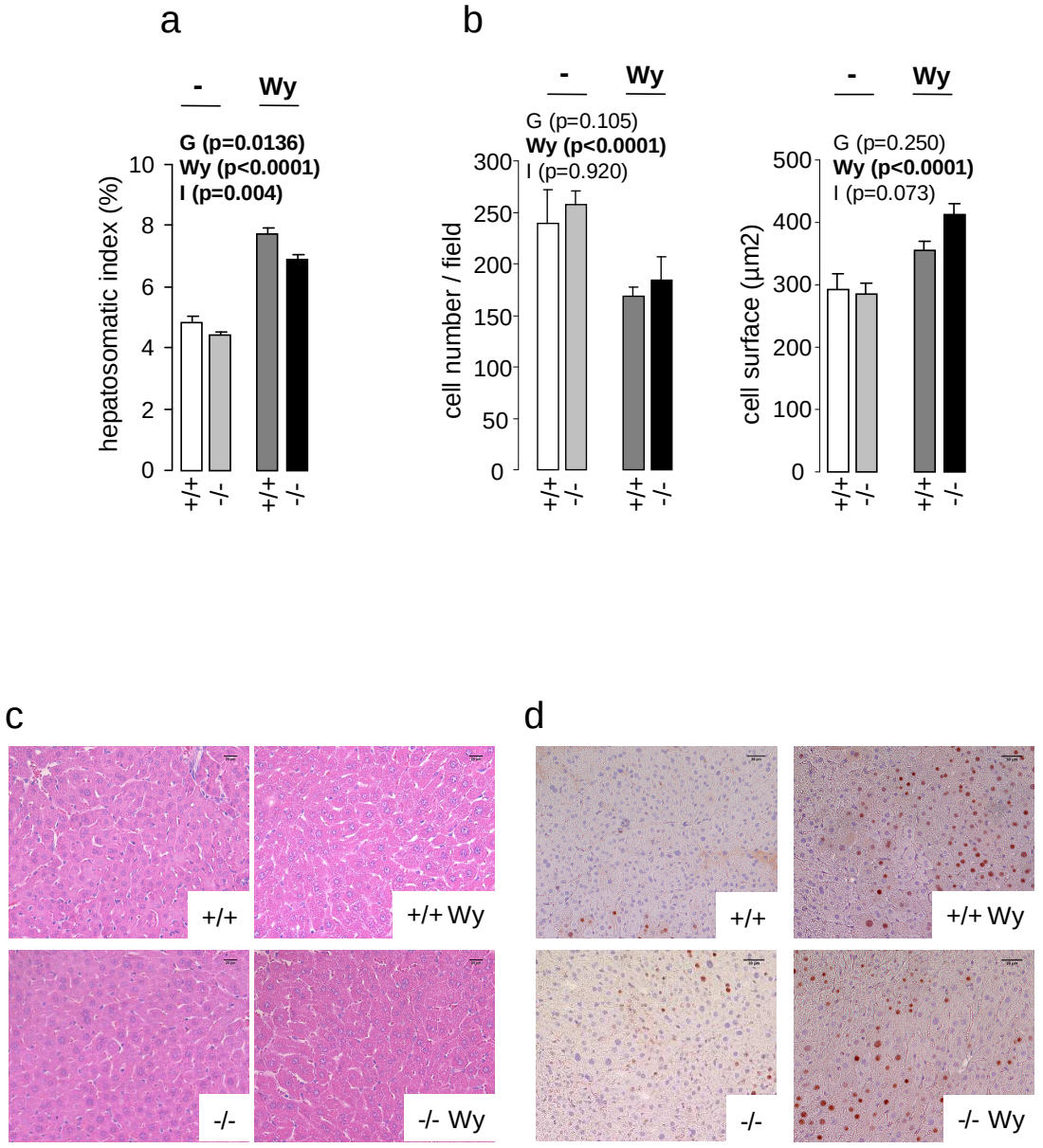

Fidaleo *et al.*, Figure 3

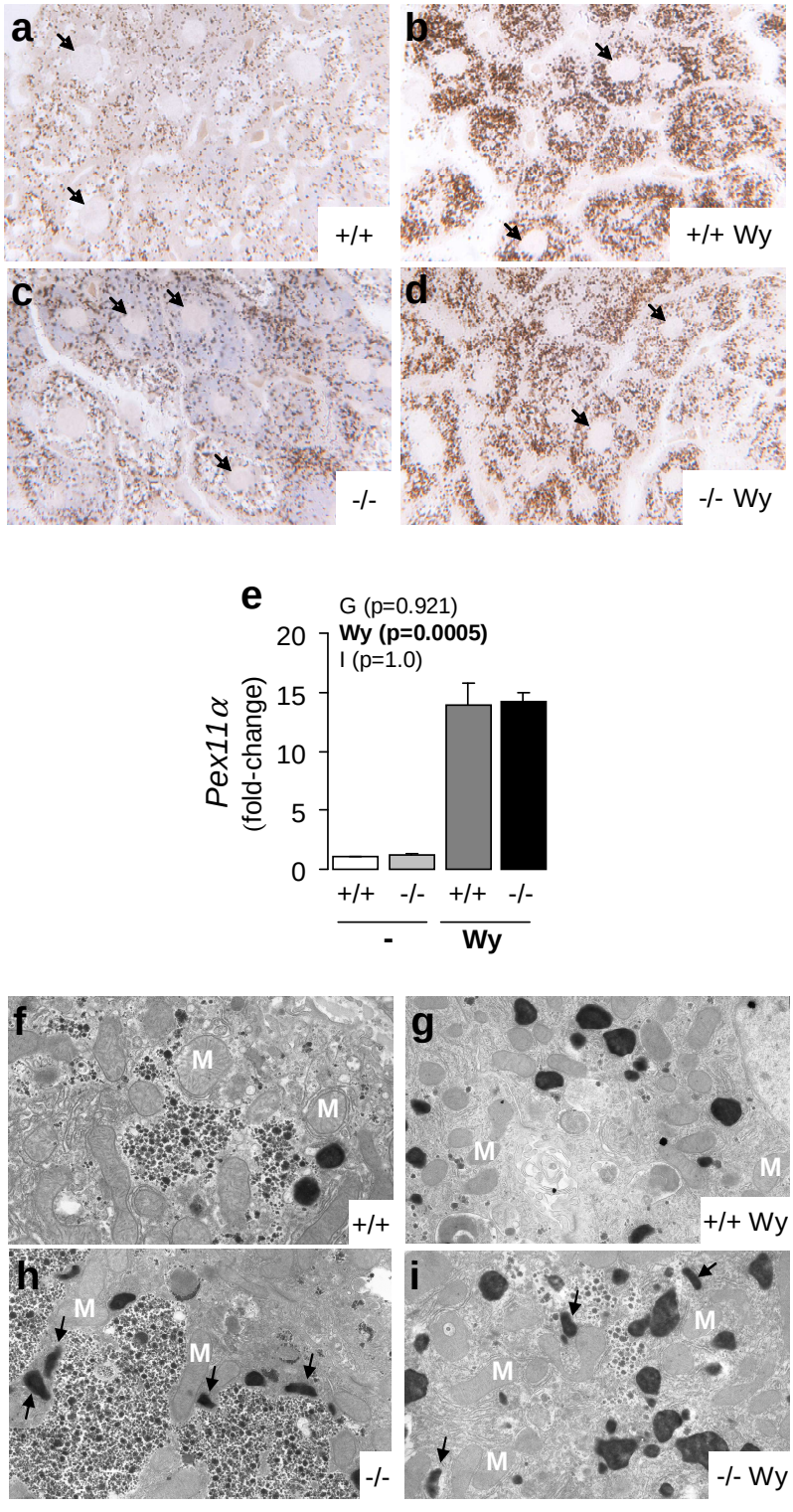

Fidaleo *et al.*, Figure 4

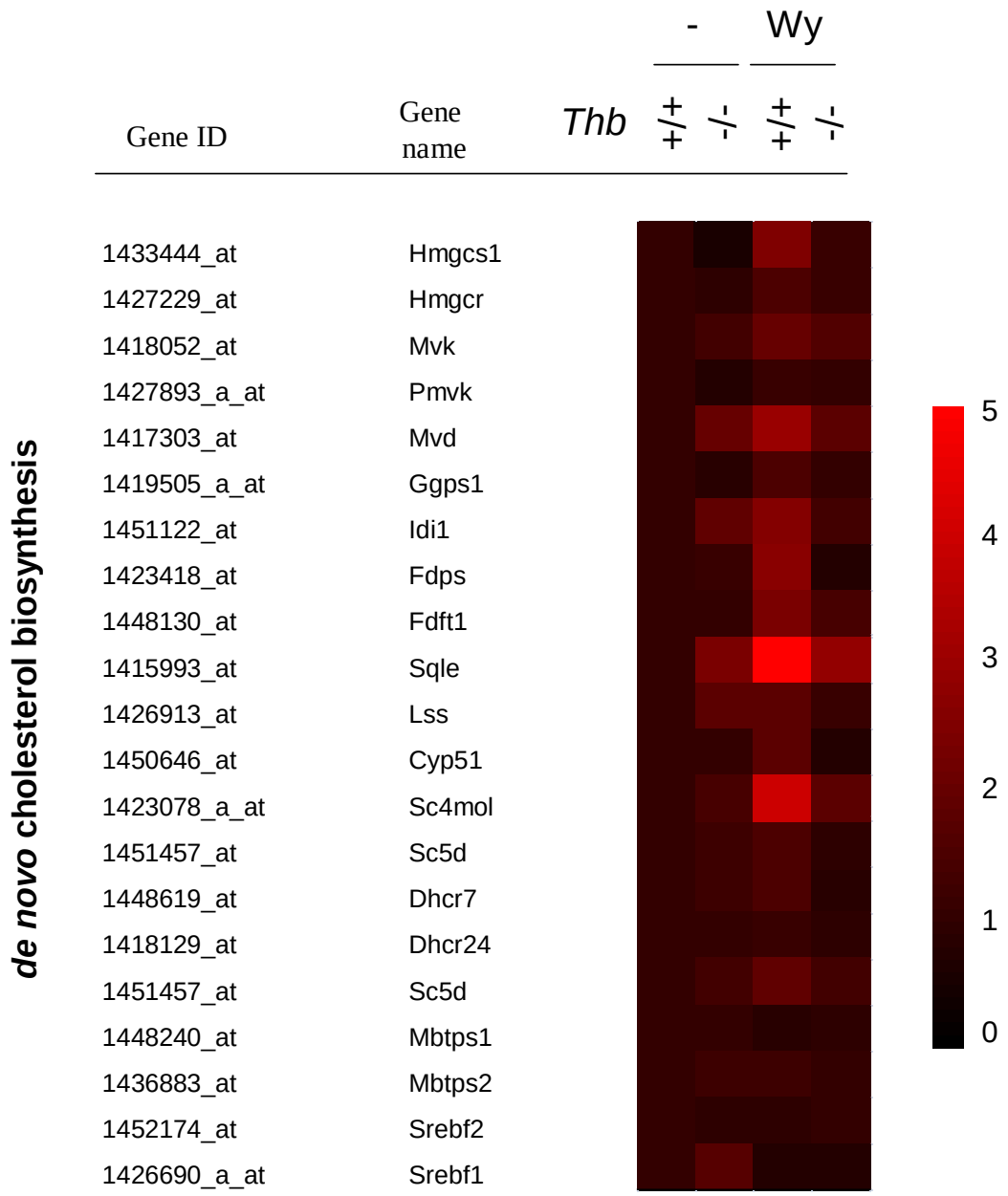

Fidaleo *et al.*, Figure 5

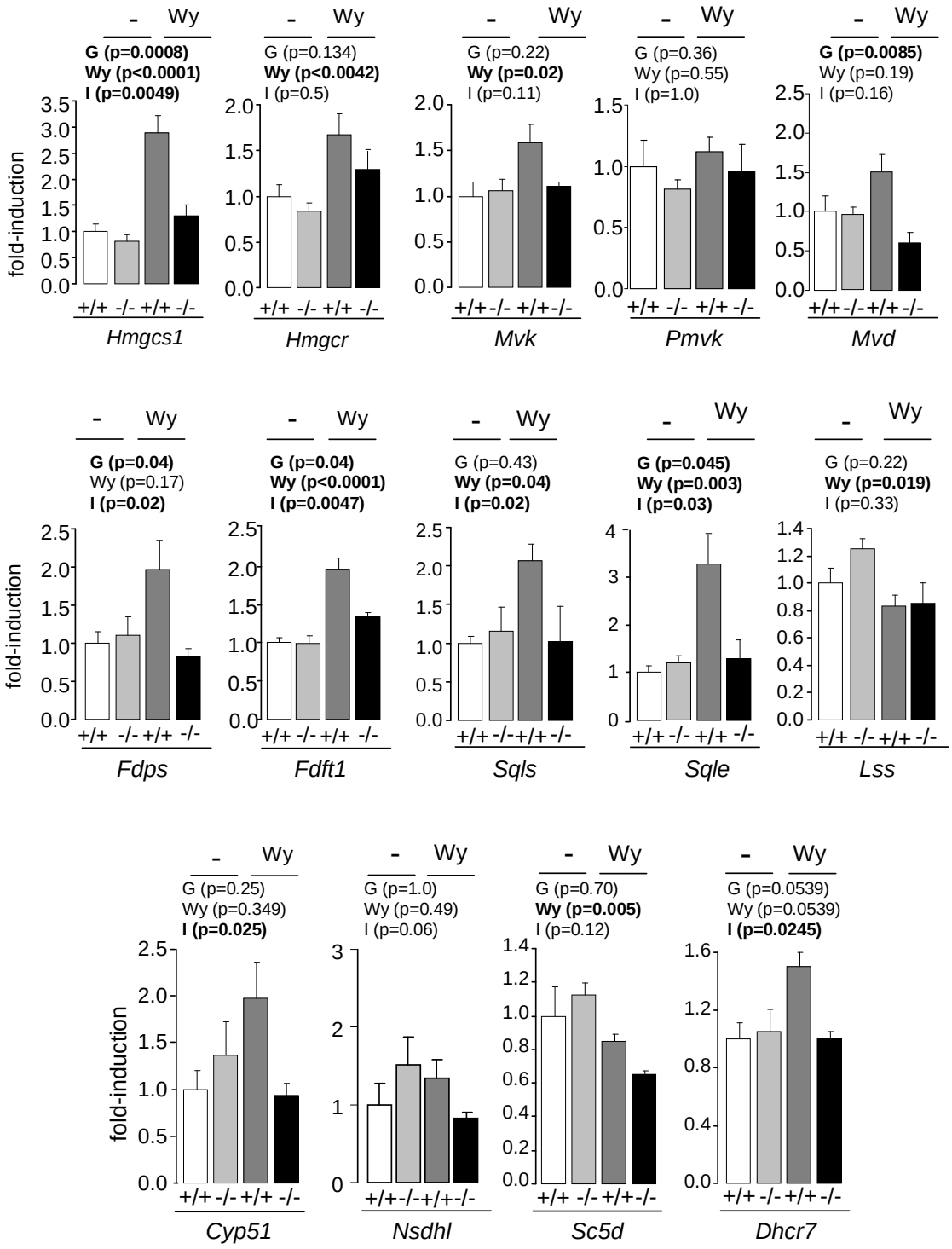

Fidaleo *et al.,* Figure 6

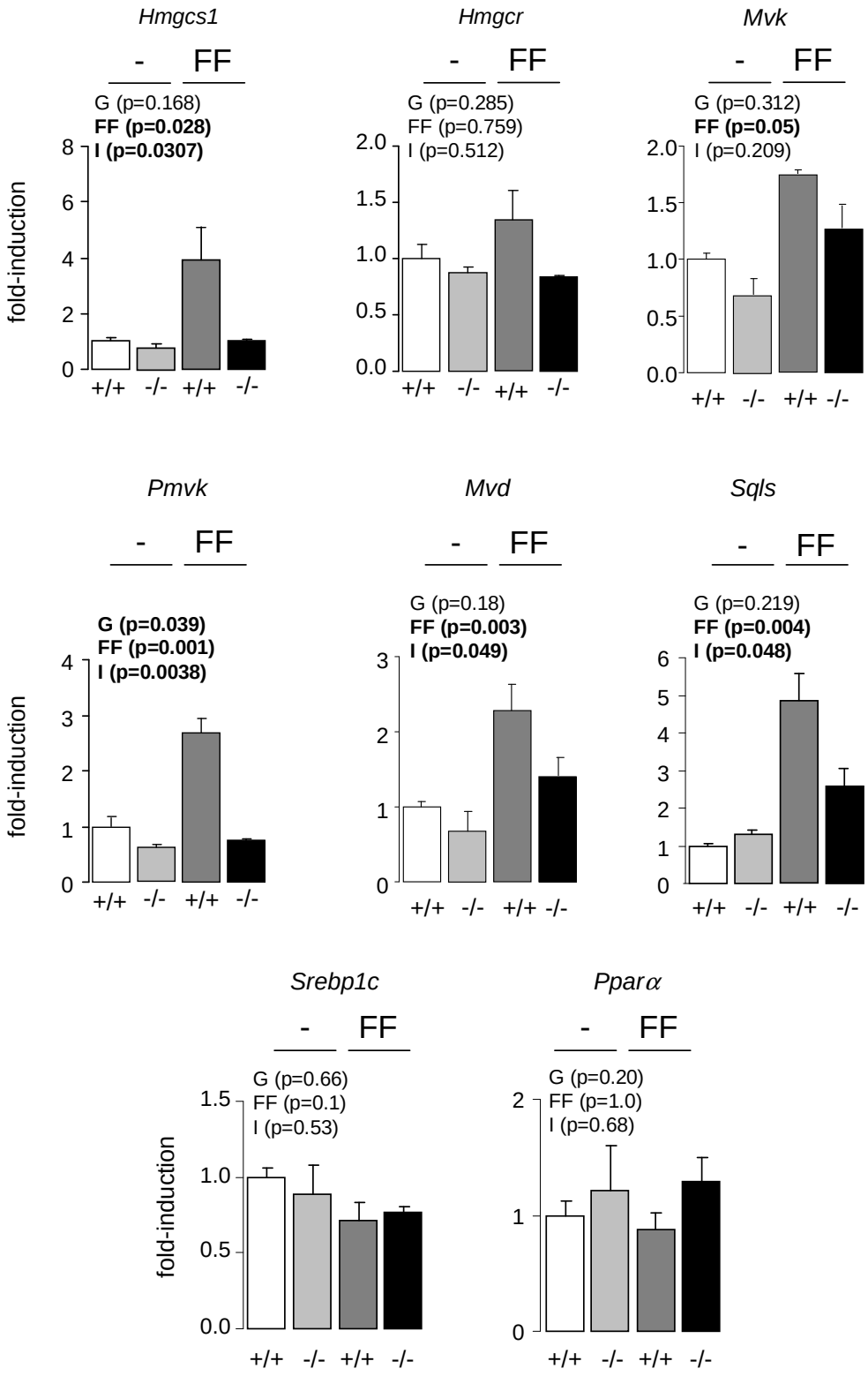

Fidaleo *et al.*, Figure 7

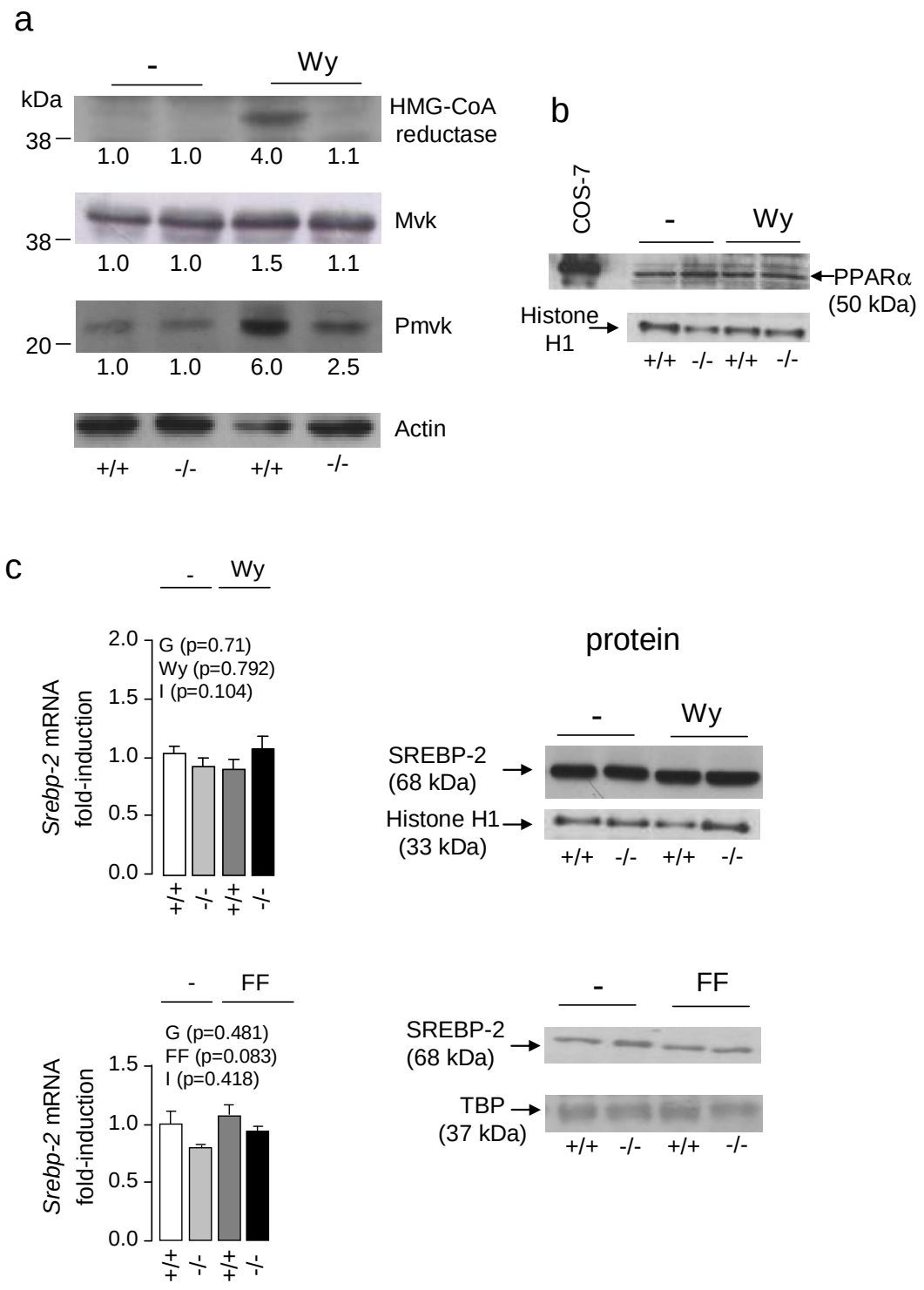

Fidaleo *et al.,* Figure 8

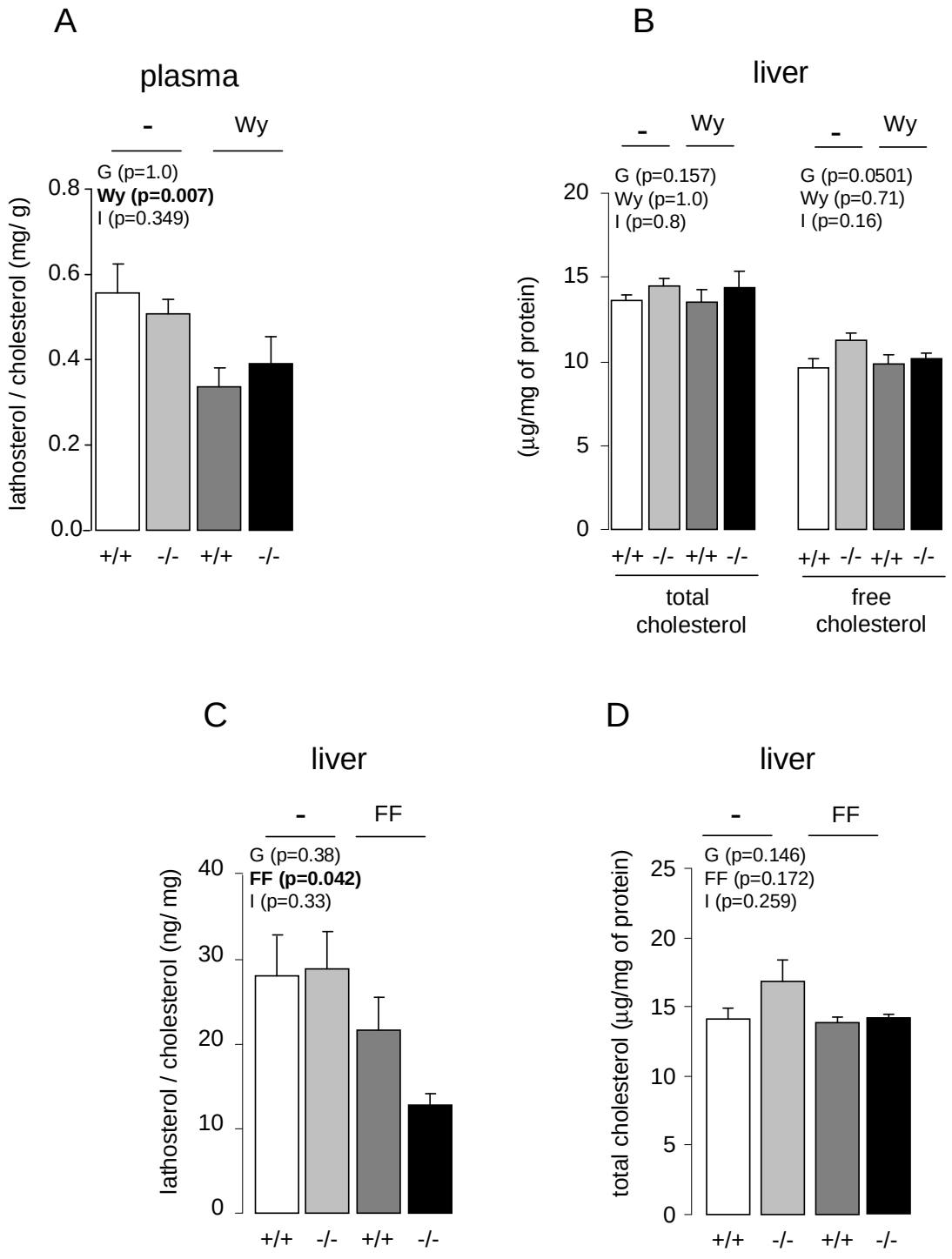

Fidaleo *et al.*, Figure 9

		-		Wy				
Genotype		**+/+**	**-/-**	**+/+**	**-/-**	Genotype (G)	Wy14,643 (Wy)	Interaction (G*Wy)
Mitochondria								
CPT-Iα activity (nmol/min/mg of mitochondrial protein)	n=3	2.5 ± 0.3	2.7 ± 0.3	3.2 ± 0.0	3.4 ± 0.5	0.63	**0.01**	1.00
monoamine oxidase (nmol/min/mg of mitochondrial protein)	n=3	6.9 ± 0.8	7.1 ± 0.5	6.4 ± 0.6	5.8 ± 0.6	0.74	0.18	0.55
citrate synthase (nmol/min/mg of mitochondrial protein)	n=3	0.22 ± 0.01	0.23 ± 0.02	0.23 ± 0.01	0.25± 0.01	1.00	1.00	1.00
*Cpt-1*α mRNA (%)	n=13	1.00 ± 0.13	0.95 ± 0.10	1.44 ± 0.13	1.51 ± 0.16	0.84	**<0.0001**	**0.04**
plasma β-hydroxybutyrate (mM)	n=13	0.34 ± 0.06	0.32 ± 0.08	0.38 ± 0.03	0.34 ± 0.1	0.63	0.63	1.00
plasma free fatty acids (mM)	n=8	0.87 ± 0.10	0.82 ± 0.06	0.51 ± 0.05	0.62 ± 0.06	0.56	**<0.0006**	0.32

		fed		24h fasting		Genotype	Fasting	Interaction
Genotype		**+/+**	**-/-**	**+/+**	**-/-**	(G)	(F)	(G*F)
plasma β-hydroxybutyrate (mM)	n=16	0.41 ± 0.04	0.41 ± 0.03	2.74 ± 0.18	2.64 ± 0.13	0.66	**<0.0001**	0.66
plasma free fatty acids (mM)	n=10	1.27 ± 0.09	1.17 ± 0.09	1.8± 0.17	1.5 ± 0.06	0.10	**0.0021**	0.37

Fidaleo *et al.*, Table 1

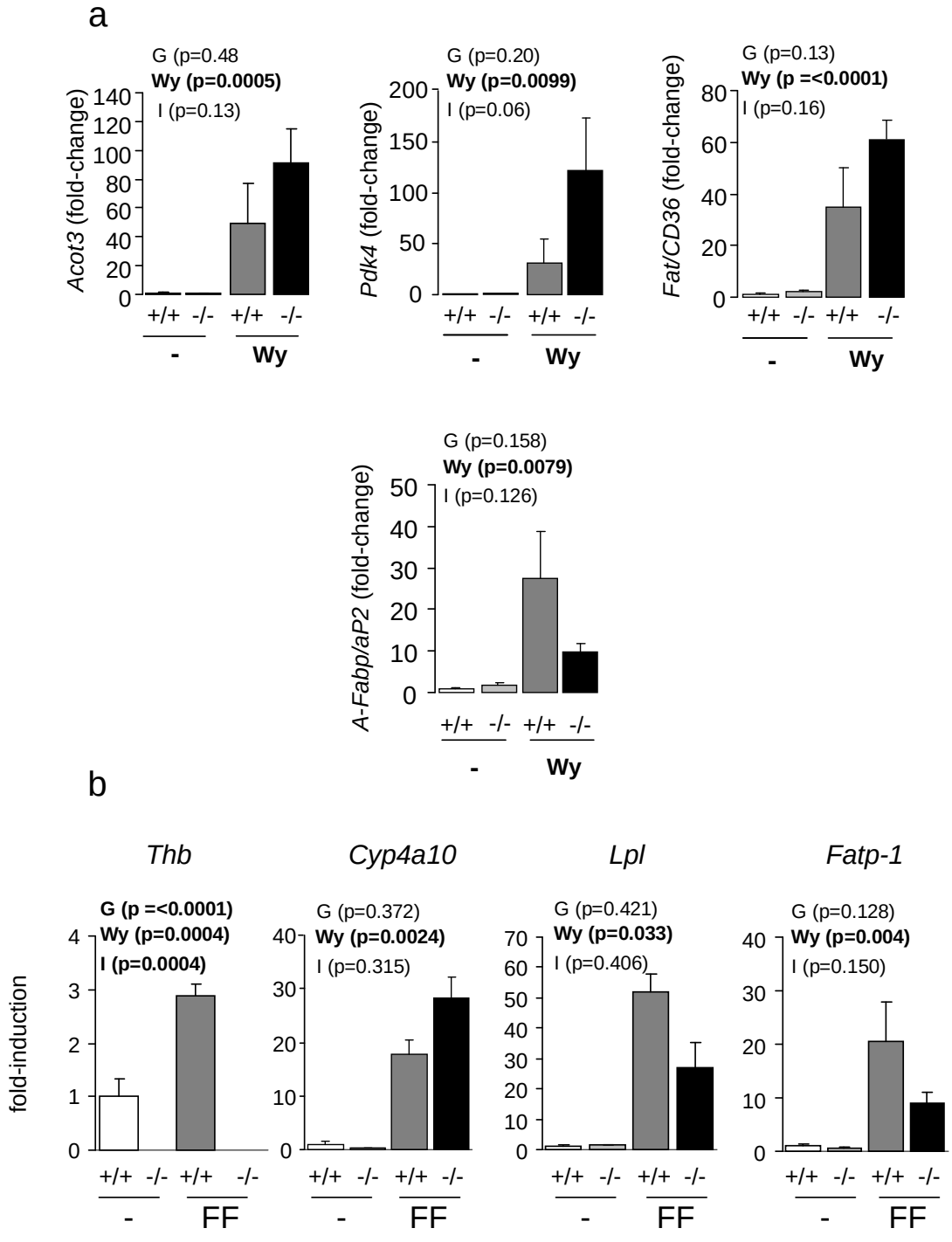

Fidaleo *et al.,* supplemental Figure 1

A	B	C	D	E	F	
		fold-change				
Probe Set ID	Gene Symbol	WT	KO	WT-Wy	KO-Wy	
Peroxisome biogenesis						
1428716_at	Pex1	1.0	1.1	1.1	1.1	peroxisome biogenesis factor 1
1454044_a_at	Pex3	1.0	1.1	1.5	1.4	peroxisomal biogenesis factor 3
1417442_a_at	Pex3	1.0	1.0	1.7	1.5	peroxisomal biogenesis factor 3
1426770_at	Pex5	1.0	1.1	1.4	1.2	peroxisome biogenesis factor 5
1422063_a_at	Pex5	1.0	1.1	1.1	1.2	peroxisome biogenesis factor 5
1424078_s_at	Pex6	1.0	0.7	0.7	0.8	peroxisomal biogenesis factor 6
1454738_x_at	Pex6	1.0	1.1	1.0	0.9	peroxisomal biogenesis factor 6
1451226_at	Pex6	1.0	1.0	0.9	1.1	peroxisomal biogenesis factor 6
1418988_at	Pex7	1.0	1.0	1.1	1.1	peroxisome biogenesis factor 7
1456646_at	Pex10	1.0	1.0	1.2	1.1	peroxisome biogenesis factor 10
1449442_at	Pex11a	1.0	0.7	1.7	2.1	peroxisomal biogenesis factor 11a
1419365_at	Pex11a	1.0	0.7	1.4	1.8	peroxisomal biogenesis factor 11a
1420460_a_at	Pex11b	1.0	1.0	1.3	1.1	peroxisomal biogenesis factor 11b
1451213_at	Pex11b	1.0	0.9	0.9	0.9	peroxisomal biogenesis factor 11b
1429407_at	Pex11c	1.0	0.7	1.1	0.9	peroxisomal biogenesis factor 11c
1430856_at	Pex11c	1.0	1.5	1.2	1.2	peroxisomal biogenesis factor 11c
1430857_s_at	Pex11c	1.0	0.8	1.1	1.1	peroxisomal biogenesis factor 11c
1416259_at	Pex12	1.0	0.9	0.9	0.9	peroxisomal biogenesis factor 12
1422471_at	Pex13	1.0	1.1	1.0	1.2	peroxisomal biogenesis factor 13
1419053_at	Pex14	1.0	0.9	1.1	1.2	peroxisomal biogenesis factor 14
1425021_a_at	Pex16	1.0	0.8	1.6	1.6	peroxisome biogenesis factor 16
1455208_at	Pex19	1.0	0.7	1.4	0.6	peroxisome biogenesis factor 19
Peroxisomal β-oxidation						
1416947_s_at	Acaa1	1.0	0.2	2.9	0.6	thiolase a & b
1416946_a_at	Acaa1	1.0	0.2	3.8	0.7	thiolase a & b
1456011_x_at	Acaa1	1.0	1.4	2.6	2.4	thiolase a
1424451_at	Acaa1	1.0	0.0	2.1	0.0	thiolase b
1416409_at	Acox1	1.0	1.0	2.9	3.3	acyl-CoA-oxidase 1
1416408_at	Acox1	1.0	0.9	2.1	2.2	acyl-CoA-oxidase 1
1448382_at	MFP-1 / L-PBE / Ehhadh	1.0	0.7	5.2	5.6	MFP-1 / L-PBE/Ehhadh
1455777_x_at	Hsd17b4/MFP-2	1.0	0.9	1.5	1.6	Hsd17b4, hydroxysteroid (17-beta) dehydrogenase 4
1417369_at	Hsd17b4/MFP-2	1.0	0.9	1.6	1.6	Hsd17b4, hydroxysteroid (17-beta) dehydrogenase 4
1448491_at	Ech1	1.0	0.7	2.3	2.6	Ech1, enoyl-COA hydratase 1
1449686_s_at	Scp2	1.0	0.9	0.9	1.0	sterol carrier protein-2
1419974_at	Scp2	1.0	2.1	1.5	4.4	sterol carrier protein-2
1426219_at	Scp2	1.0	1.1	1.1	1.2	sterol carrier protein-2
1420673_a_at	Acox2	1.0	1.1	1.2	1.4	acyl-Coenzyme A oxidase 2, branched chain
1422604_at	Uox	1.0	1.1	1.0	1.0	urate oxidase
1416679_at	Abcd3	1.0	0.9	1.5	1.6	PMP70/ABCD3
1416430_at	Cat	1.0	0.9	0.9	0.9	catalase
1416429_a_at	Cat	1.0	1.0	0.9	0.9	catalase
1422925_s_at	Acot3	1.0	1.0	7.8	7.3	acyl-CoA thioesterase 3
1417449_at	Acot8	1.0	0.6	2.0	1.9	acyl-CoA thioesterase 8

Fidaleo *et al.*, Supplemental Table 1

A	B	C	D	E	F	
		fold-change				
Probe Set ID	Gene Symbol	WT	KO	WT-Wy	KO-Wy	
Mitochondrial β-oxidation and markers						
1438156_x_at	Cpt1a	1.0	0.9	1.2	1.6	carnitine palmitoyltransferase 1a, liver
1434866_x_at	Cpt1a	1.0	0.9	1.2	1.6	carnitine palmitoyltransferase 1a, liver
1460409_at	Cpt1a	1.0	0.9	1.6	2.0	carnitine palmitoyltransferase 1a, liver
1418321_at	Cpt2	1.0	0.8	2.4	2.5	carnitine palmitoyltransferase 2
1419367_at	Decr1	1.0	0.8	2.4	2.8	2,4-dienoyl CoA reductase 1, mitochondrial
1449443_at	Decr1	1.0	0.8	1.6	2.2	2,4-dienoyl CoA reductase 1, mitochondrial
1452173_at	Hadha	1.0	0.9	1.9	2.1	hydroxyacyl-Coenzyme A dehydrogenase/3-ketoacyl-Coenzyme A thiolase/enoyl-Coen
1426522_at	Hadhb	1.0	0.8	2.1	2.2	hydroxyacyl-Coenzyme A dehydrogenase/3-ketoacyl-Coenzyme A thiolase/enoyl-Coen
1460184_at	Hadhsc	1.0	1.1	1.6	1.7	L-3-hydroxyacyl-Coenzyme A dehydrogenase, short chain
1460216_at	Acads	1.0	0.7	2.1	1.2	acyl-Coenzyme A dehydrogenase, short chain
1448987_at	Acadl	1.0	0.9	2.0	2.1	acetyl-Coenzyme A dehydrogenase, long-chain
1424184_at	Acadvl	1.0	1.0	1.4	1.7	acyl-Coenzyme A dehydrogenase, very long chain
1423108_at	Slc25a20	1.0	0.8	1.7	1.8	solute carrier family 25 (mitochondrial carnitine/acylcarnitine translocase), member 20
1423109_s_at	Slc25a20	1.0	0.8	1.7	1.7	solute carrier family 25 (mitochondrial carnitine/acylcarnitine translocase), member 20
1424639_a_at	Hmgcl	1.0	1.0	1.6	1.9	3-hydroxy-3-methylglutaryl-Coenzyme A lyase
1431833_a_at	Hmgcs2	1.0	0.9	1.1	1.4	3-hydroxy-3-methylglutaryl-Coenzyme A synthase 2
1423858_a_at	Hmgcs2	1.0	0.7	1.3	1.3	3-hydroxy-3-methylglutaryl-Coenzyme A synthase 2
1422578_at	Cs	1.0	1.0	1.0	0.9	citrate synthase
1450667_a_at	Cs	1.0	1.0	0.9	0.9	citrate synthase
1428667_at	Maoa	1.0	1.4	1.6	1.7	monoamine oxidase A
1434354_at	Maob	1.0	1.2	1.1	1.1	monoamine oxidase B
Microsomal ω-oxidation						
1423257_at	Cyp4a14	1.0	0.3	1.6	1.7	cytochrome P450, family 4, subfamily a, polypeptide 14
1424943_at	Cyp4a10	1.0	0.3	11.1	11.1	cytochrome P450, family 4, subfamily a, polypeptide 10
1415776_at	Aldh3a2	1.0	0.9	3.0	3.9	aldehyde dehydrogenase family 3, subfamily A2
Cell cycle/cell proliferation						
1448698_at	Ccdn1	1.0	1.1	0.6	0.8	cyclin D1
1417420_at	Ccdn1	1.0	1.0	0.6	0.8	cyclin D1
1416122_at	Ccdn2	1.0	1.2	0.7	0.9	cyclin D2
1448364_at	Ccdn2	1.0	1.0	0.7	0.7	cyclin D2
1416488_at	Ccng2	1.0	0.7	1.4	1.6	cyclin G2
1448364_at	Ccng2	1.0	0.8	2.2	2.0	cyclin G2
1424001_at	Mki67ip	1.0	1.1	1.1	1.3	Mki67 (FHA domain) interacting nucleolar phosphoprotein
1427005_at	Plk2	1.0	0.8	0.7	0.5	polo-like kinase 2 (Drosophila)
1434496_at	Plk3	1.0	0.5	1.4	2.1	polo-like kinase 3 (Drosophila)
1416868_at	Cdkn2c	1.0	1.2	1.5	1.2	cyclin-dependent kinase inhibitor 2C
1437580_s_at	Nek2	1.0	1.2	1.6	1.7	NIMA (never in mitosis gene a)- related expressed kinase 2
1452040_a_at	Cdca3	1.0	1.3	2.2	1.9	cell division cycle associated 3
1452040_a_at	Tde2l	1.0	0.7	26	12	tumor differentially expressed 2-like
Pro-apoptotic genes						
1450971_at	Gadd45b	1.0	0.5	4.6	3.3	growth arrest and DNA-damage- inducible 45 beta
1416837_at	Bax	1.0	0.9	1.2	0.7	Bcl2-associated X protein
Anti-apoptotic genes						
1418528_at	Dad1	1.0	0.8	0.7	0.6	defender against cell death 1

A	B	C	D	E	F	
		fold-change				
Probe Set ID	Gene Symbol	WT	KO	WT-Wy	KO-Wy	
***De novo* cholesterol biosynthesis**						
1433445_x_at	Hmgcs1	1.0	0.7	2.3	1.2	3-hydroxy-3-methylglutaryl-Coenzyme A synthase 1
1433443_a_at	Hmgcs1	1.0	0.7	2.5	1.3	3-hydroxy-3-methylglutaryl-Coenzyme A synthase 1
1433444_at	Hmgcs1	1.0	0.5	2.5	1.1	3-hydroxy-3-methylglutaryl-Coenzyme A synthase 1
1433446_at	Hmgcs1	1.0	0.6	2.0	1.1	3-hydroxy-3-methylglutaryl-Coenzyme A synthase 1
1427229_at	Hmgcr	1.0	0.9	1.5	1.1	3-hydroxy-3-methylglutaryl-Coenzyme A reductase
1418052_at	Mvk	1.0	1.3	2.0	1.6	mevalonate kinase
1427893_a_at	Pmvk	1.0	0.7	1.1	1.0	phosphomevalonate kinase
1448663_s_at	Mvd	1.0	1.3	2.5	0.6	mevalonate (diphospho) decarboxylase
1417303_at	Mvd	1.0	2.0	3.0	1.8	mevalonate (diphospho) decarboxylase
1419805_s_at	Ggps1	1.0	0.9	1.0	0.9	geranylgeranyl diphosphate synthase 1
1419505_a_at	Ggps1	1.0	0.8	1.5	1.0	geranylgeranyl diphosphate synthase 1
1451122_at	Idi1	1.0	1.9	2.6	1.3	isopentenyl-diphosphate delta isomerase
1423418_at	Fdps	1.0	1.1	2.7	0.7	farnesyl diphosphate synthetase
1438322_x_at	Fdft1	1.0	1.1	2.0	1.2	farnesyl diphosphate farnesyl transferase 1
1448130_at	Fdft1	1.0	1.0	2.4	1.4	farnesyl diphosphate farnesyl transferase 1
1415993_at	Sqle	1.0	2.4	6.4	2.9	squalene epoxidase
1420013_s_at	Lss	1.0	1.6	2.3	1.5	lanosterol synthase
1426913_at	Lss	1.0	1.8	1.8	1.1	lanosterol synthase
1450646_at	Cyp51	1.0	1.0	1.8	0.7	cytochrome P450, family 51; lanosterol 14α-demethylase
1423078_a_at	Sc4mol	1.0	1.4	4.0	1.8	sterol-C4-methyl oxidase-like
1424709_at	Sc5d	1.0	0.8	0.9	0.7	sterol-C5-desaturase (fungal ERG3, delta-5-desaturase) homolog (S. cerevisae)
1434520_at	Sc5d	1.0	1.1	0.7	0.6	sterol-C5-desaturase (fungal ERG3, delta-5-desaturase) homolog (S. cerevisae)
1451457_at	Sc5d	1.0	0.8	0.8	0.5	sterol-C5-desaturase (fungal ERG3, delta-5-desaturase) homolog (S. cerevisae)
1448619_at	Dhcr7	1.0	1.0	1.1	0.9	7-dehydrocholesterol reductase
1451895_a_at	Dhcr24	1.0	1.1	1.7	1.6	24-dehydrocholesterol reductase / 3β-hydroxysterol-Δ24 reductase (seladin-1)
1418130_at	Dhcr24	1.0	1.3	1.8	1.4	24-dehydrocholesterol reductase / 3β-hydroxysterol-Δ24 reductase (seladin-1)
1418129_at	Dhcr24	1.0	1.3	1.9	1.3	24-dehydrocholesterol reductase / 3β-hydroxysterol-Δ24 reductase (seladin-1)
1416222_at	Nsdhl	1.0	1.2	1.5	0.9	NAD(P) dependent steroid dehydrogenase-like
1448240_at	Mbtps1	1.0	1.0	0.8	0.9	membrane-bound transcription factor peptidase, site 1
1431385_a_at	Mbtps1	1.0	1.0	0.8	1.0	membrane-bound transcription factor peptidase, site 1
1436883_at	Mbtps2	1.0	1.2	1.2	1.0	membrane-bound transcription factor peptidase, site 2
1426690_a_at	Srebf1	1.0	1.7	0.7	0.7	sterol regulatory element binding factor 1
1452174_at	Srebf2	1.0	0.9	0.9	1.0	sterol regulatory element binding factor 2
1433520_at	Scap	1.0	1.0	1.2	1.3	SREBP cleavage activating protein
1454671_at	Insig1	1.0	1.3	1.1	0.8	insulin induced gene 1
1417980_a_at	Insig2	1.0	0.7	1.3	1.3	insulin induced gene 2
1417982_at	Insig2	1.0	0.8	1.1	1.2	insulin induced gene 2

NB: Squalene synthase was not present on the arrays.

Fidaleo *et al*., Supplemental Table 1

A	B	C	D	E	F	
		fold-change				
Probe Set ID	Gene Symbol	WT	KO	WT-Wy	KO-Wy	
Sterol transport/trafficking						
1421840_at	Abca1	1.0	1.0	1.2	1.1	ATP-binding cassette, sub-family A (ABC1), member 1
1421839_at	Abca1	1.0	0.9	1.2	1.0	ATP-binding cassette, sub-family A (ABC1), member 1
1419393_at	Abcg5	1.0	1.5	1.2	1.5	ATP-binding cassette, sub-family G (WHITE), member 5
1420656_at	Abcg8	1.0	1.4	1.0	1.1	ATP-binding cassette, sub-family G (WHITE), member 8
1449817_at	Abcb11	1.0	1.2	0.4	0.5	ATP-binding cassette, sub-family B (MDR/TAP), member 11
1421821_at	Ldlr	1.0	1.2	1.1	0.9	low density lipoprotein receptor
1437453_s_at	Pcsk9	1.0	1.8	2.5	1.2	proprotein convertase subtilisin/kexin type 9
1423086_at	Npc1	1.0	1.1	1.1	0.9	Niemann Pick type C1
1448513_a_at	Npc2	1.0	1.0	0.8	0.7	Niemann Pick type C2
1416901_at	Npc2	1.0	1.0	1.0	0.8	Niemann Pick type C2
Nuclear hormone receptors (towards lipid metabolism)						
1449051_at	Nr1c1-Pparα	1.0	1.5	1.3	1.5	peroxisome proliferator activated receptor alpha
1416353_at	Nr1h2-Lxrβ	1.0	0.9	0.8	0.7	nuclear receptor subfamily 1, group H, member 2
1450444_a_at	Nr1h3-Lxrα	1.0	0.8	0.8	0.9	nuclear receptor subfamily 1, group H, member 3
1419105_at	Nr1h4-Fxrα	1.0	0.8	0.8	0.8	nuclear receptor subfamily 1, group H, member 4
1449854_at	Nr0b2-Shp	1.0	0.8	0.6	1.1	nuclear receptor subfamily 0, group B, member 2
1429382_at	Nr1i3-Car	1.0	1.0	1.4	1.7	nuclear receptor subfamily 1, group I, member 3
1455614_at	Nr1i3-Car	1.0	0.7	1.1	1.0	nuclear receptor subfamily 1, group I, member 3
SREBP interacting protein						
1449945_at	Ppargc1b	1.0	1.2	0.9	1.0	peroxisome proliferative activated receptor, gamma, coactivator 1 beta
1434633_at	Crebbp	1.0	0.9	1.0	0.8	CREB binding protein
1420410_at	Nr5a2-Lrh1	1.0	2.4	1.4	1.6	nuclear receptor subfamily 5, group A, member 2
1449706_s_at	Nr5a2-Lrh1	1.0	1.4	1.1	1.3	nuclear receptor subfamily 5, group A, member 2
1456021_at	Atf6	1.0	0.7	1.0	1.0	activating transcription factor 6
1435444_at	Atf6	1.0	0.8	0.7	0.6	activating transcription factor 6
1450447_at	Nr2a1-Hnf4α	1.0	1.3	1.4	1.7	nuclear receptor subfamily 2, group A, member 1
1427001_s_at	Nr2a1-Hnf4α	1.0	1.0	0.9	1.1	nuclear receptor subfamily 2, group A, member 1
1421983_s_at	Nr2a1-Hnf4α	1.0	1.1	0.9	1.1	nuclear receptor subfamily 2, group A, member 1
1427000_at	Nr2a1-Hnf4α	1.0	0.9	1.0	1.0	nuclear receptor subfamily 2, group A, member 1
Protein modification of SREBP						
1454958_at	Gsk3b	1.0	1.1	1.0	1.0	glycogen synthase kinase 3 beta
1439949_at	Gsk3b	1.0	1.0	1.0	1.0	glycogen synthase kinase 3 beta
1448174_at	Cul1	1.0	0.9	0.9	0.8	cullin 1
1416577_a_at	Rbx1	1.0	0.9	0.8	0.9	ring-box 1
1448387_at	Rbx1	1.0	1.1	0.9	1.0	ring-box 1
Miscellaneous (towards PPARalpha regulated genes)						
1423166_at	Cd36	1.0	0.9	9.6	10.3	CD36 antigen
1450883_a_at	Cd36	1.0	0.9	9.5	9.0	CD36 antigen
1450884_at	Cd36	1.0	0.8	6.9	6.6	CD36 antigen
1417023_a_at	Fabp4	1.0	1.3	25.4	10.0	fatty acid binding protein 4, adipocyte
1415904_at	Lpl	1.0	1.9	5.6	6.0	lipoprotein lipase
1431056_a_at	Lpl	1.0	2.2	5.9	4.7	lipoprotein lipase
1456424_s_at	Pltp	1.0	1.0	3.6	3.0	phospholipid transfer protein
1417963_at	Pltp	1.0	0.7	4.0	3.5	phospholipid transfer protein
1417273_at	Pdk4	1.0	0.7	7.0	4.0	pyruvate dehydrogenase kinase, isoenzyme 4
1422076_at	Acot4	1.0	1.0	2.9	3.7	acyl-CoA thioesterase 4
1422997_s_at	Acot1 /// Acot2	1.0	0.5	11.4	13.2	acyl-CoA thioesterase 1 /// acyl-CoA thioesterase 2
1439478_at	Acot2	1.0	0.6	2.6	2.4	acyl-CoA thioesterase 2

Fidaleo *et al*., Supplemental Table 1

Gene	forward primer	reverse primer
Thb	ATCCGGTTCTCTCGGTCGA	TGTGGTCAAGCATAGCATGCA
Tha	CCTGAACAGTGCTGAAGTGAG	ACAGTACACATTTACTGCATCCC
Mfp-1	AAGCCATTGCCAAGGTACGGAAG	GCCTGGACTGAACGGACACAAG
Scpx/Scp2	GTCTCGTCGTCAGGGCTTAG	TTGACCACACCCAATTAGCA
Acox-I	GCCCAACTGTGACTTCCATT	GGCATGTAACCCGTAGCACT
Acot3	TCCAACATCGGCGGAAACTTA	ACGGGAATCAAGCTCTTCTGG
Pdk4	CCGCTTAGTGAACACTCCTTC	TCTACAAACTCTGACAGGGCTTT
Fat/Cd36	ATGGGCTGTGATCGGAACTG	GTCTTCCCAATAAGCATGTCTCC
Cpt1α	CTCAGTGGGAGCGACTCTTCA	GGCCTCTGTGGTACACGACAA
Cdk1	ATGATCCTGCCAAACGAATC	TCCATCCAGAGGGCTACATC
Cdk4	TGCCAGAGATGGAGGAGTCT	TTGTGCAGGTAGGAGTGCTG
Cdk1a/p21	GCTCACAGGACACTGAGCAA	GCTTTGACACCCACGGTATT
Pcna	TTGGAATCCCAGAACAGGAG	GTGGCTAAGGTCTCGGCATA
Pex11alpha	ACTGGCCGTAAATGGTTCAGA	CGGTTGAGGTTGGCTAATGTC
HMG-CoA synthase	GTGGCACCGGATGTCTTTG	ACTCTGACCAGATACCACGTT
HMG-CoA reductase	AGCTTGCCCGAATTGTATGTG	TCTGTTGTGAACCATGTGACTTC
Phosphomevalonate kinase	CATTGAGAACCACGGAGATG	CATCTGGCAGAACCACTGTT
Farnesyl diphosphate synthase	GGAGGTCCTAGAGTACAATGCC	AAGCCTGGAGCAGTTCTACAC
Farnesyl diphosphate farnesyl transferase-1	TCCCACTGCTGTGTAACTTCC	TGTCTACAAATTCTGCCATCCC
Squalene synthase	TCCCACTGCTGTGTAACTTCC	TGTCTACAAATTCTGCCATCCC
Squalene epoxidase	ATAAGAAATGCGGGGATGTCAC	ATATCCGAGAAGGCAGCGAAC
Lanosterol synthase	CAGCAGTGAGAGACCTGGAA	AGAAGCGTTGATGTGACTGG
Lanosterol-14alpha demethylase (CYP51)	CTGAGAAGCTCTCGTGCTGT	TTCAAATGCCATTCGGTCT
Steroid 5-alpha reductase 1	TGAGTGTCATGCTGAGGGAT	TGTCGGACAATTAACCAAGC
7-alpha dehydrocholesterol reductase	ACCTAGCAGCTCATCCACCT	CTAAGGCCACTGACTGGTGA
Srebp-2	CTGCAGCCTCAAGTGCAAAG	CAGTGTGCCATTGGCTGTCT
36b4	ATGGGTACAAGCGCGTCCTG	GCCTTGACCTTTTCAGTAAG

Fidaleo *et al.*, Supplemental Table 2